SLAC-203
UC-34d
(T/E)

RELATIVISTIC INTERACTIONS IN NUCLEI AND THE APPROACH TO SCALING IN DEEP INELASTIC SCATTERING*

IVAN A. SCHMIDT

STANFORD LINEAR ACCELERATOR CENTER

STANFORD UNIVERSITY

Stanford, California 94305

PREPARED FOR THE ENERGY RESEARCH AND DEVELOPMENT ADMINISTRATION

UNDER CONTRACT NO. EY-76-C-03-0515

August 1977

Printed in the United States of America. Available from National Technical Information Service, U.S. Department of Commerce, 5285 Port Royal Road, Springfield, VA 22161. Price: Printed Copy $5.00; Microfiche $3.00.

*Ph.D. dissertation.

ABSTRACT

A relativistic theory of the inclusive scattering of nuclei is given. The theory is applicable to meson production reactions as well as to the yields of light nuclei. A characterization of the relativistic nuclear wave function is given and its connection to the standard wave function is explicitly shown. Counting rules are derived that allow one to simply characterize the behavior of the reaction cross sections in terms of the short range behavior of the nucleon-nucleon force. Good agreement with experiment is achieved if the force is assumed to be due to the exchange of vector mesons with monopole form factors at each vertex. The predictions are successfully compared to several reactions. The theory can also be applied to electromagnetic interactions in light nuclei. Using our relativistic nuclear wave functions, form factors and deep inelastic structure functions are analyzed.

A simple parton-model interpretation of the approach to scaling observed in lepton scattering off protons and deuterons is also presented. Different final state configurations are classified and their behavior predicted using quark counting rules. Good fits to the proton data are obtained. An extraction of the neutron structure function is performed by fitting the deuteron data. Several characteristics of the resulting parametrizations are shown to support our general model. Further experimental consequences are described.

Acknowledgements

It is a real pleasure to thank in a very special way my advisor, Professor R. Blankenbecler, for all the help and assistance that he gave me during the development of this dissertation. I feel very fortunate to have had the opportunity to learn and work with him during this period of my life.

I am also grateful to Professor S.J. Brodsky for his continuous encouragement, and for many helpful discussions and suggestions.

There are several other persons that in one way or another have helped me during this period, and I would like to name some of them: M. Aelion, A. Fernández-Pacheco, J.A. Grifols, P. Lepage, B. Pire, J. Sapirstein, R. Suaya and E. Zeiger. To all of them, and also to my friends at the Universidad Técnica Federico Santa María (Valparaíso, Chile), my sincere gratitude.

Finally, and most important of all, this work is dedicated to my father, Eugenio Schmidt. He knows very well the reasons for all my love and gratitude.

TABLE OF CONTENTS

LIST OF FIGURES

CHAPTER 1. INTRODUCTION

The theoretical description of reactions of systems with baryon number equal to one and zero has been usually very different from that of systems with larger baryon number. Historically this situation reflects itself in the separate development of two areas of physics, called respectively particle physics and nuclear physics.

The methods used in nuclear physics have had a remarkable success in describing static properties of nuclei and reactions at reasonable low energies. In the mean time, the requirements of special relativity and nonconservation of number of particles at high energies made the development of particle physics quite different from that of nuclear physics.

There is one place in which these two areas of physics meet quite naturally, and that place is high energy interactions of nuclei. In fact, recent experiments[1-5] using very high energy ion beams have already created great theoretical activity[6-10] and many ideas that had been previously applied to hadron collisions are being tested and confronted with these new data.

Probably the most successful set of models for scattering of hadrons are the relativistic hard-collision models,[11] based on a form of the impulse approximation. Here the colliding hadrons emit virtual sub-systems, which are in the end the ones responsible for the scattering process to occur. One of the purposes of this thesis is to generalize this model to high energy interactions of nuclei.

It is interesting to recall the origins of these hard-collision models. They are an extension of the parton model ideas of composite hadrons. In

the original parton model, a hadron is considered composed of elementary constituents called partons, and this idea was conceived having in mind the analogous situation in which a nucleus is composed by nucleons. So what we want to do is to apply this model to the nuclear case, where it had its origins in the first place. The important point is that we can incorporate in a natural way the key elements of special relativity and nonconservation of number of particles.

We expect our generalization to work reasonably well, because in the nuclear case the characteristics of the constituents (nucleons) are well known. On the other hand, it is clear that it must work with sufficiently general wavefunctions and interactions, so our purpose is to find a reasonably simple description of the process and of the main results.

Perhaps our most important formula for the inclusive scattering of nuclei is

$$R_c = I(\varepsilon)\ \varepsilon^{F+1+H}\ (1 - x_R \cos\theta_{cm})^{-F_-}(1 + x_R \cos\theta_{cm})^{-F_+}\ J(C_T^2) \quad ,$$

which characterizes the behavior of the cross section for all angles. The powers F, F_+, F_-, H can be calculated using very simple rules (see section (III.1C) for definitions and details).

One important restriction that we face is that our model must have a correct nonrelativistic limit, that is, it must join in this limit with the usual nuclear physics description based on Schrödinger wavefunctions and interactions. This connection will provide us with useful information on the parameters of our relativistic model. It is important to stress the fact that the model contains the usual nonrelativistic results, provided appropriate wavefunctions with correct limits are incorporated. However,

since we will concentrate for the most part on the kinematic regime that explores the short distance behavior of the nuclear wavefunction, we will obtain new information that is not accessible from the nonrelativistic description.

The model is quite general, and in fact should be applicable to the relativistic scattering of almost any composite system, provided the impulse approximation is a reasonable one for the situation under consideration, and provided correct wavefunctions and interactions are inserted. However, since the model is based on the impulse approximation, in which the effects of rescattering and shadowing are neglected, our analysis should be most applicable to light nuclei. This also means that we will not try to explain the anomalous dependence on nucleon number observed in large transverse events,[12] which is presumably connected to the effects mentioned before.

As we have said, our treatment will be fully relativistic. On the other hand, some effects due to the creation and destruction of particles will be neglected, which means that although we are working at high energy so that a relativistic analysis is necessary, it is still not too high for all the effects due to the nonconservation of the number of particles to be important. In parton model language, the "sea", which corresponds to the virtual pionic cloud in the nuclear case, will be neglected.

The model is not only applicable to strong interactions, but also to electromagnetic and weak interactions in nuclei. In fact, the fourth chapter of this thesis contains applications to the electromagnetic case. First the form factors of several light nuclei are computed, and then we present a detailed analysis of deep inelastic scattering off deuterons. The study of weak interactions in nuclei can be handled in an analogous fashion.

One of the important lessons that we will be able to learn from the analysis of nuclear scattering is that there are terms which dominate in certain regions of phase space, and which correspond to scattering of coherent sub-systems emitted by the nucleus (deuterons, α-particles, etc.). It is interesting to note that in the CIM model for the scattering of hadrons[11] this same coherence idea appears, and it is quite successful in interpreting the experimental data, specially at high transverse momentum.

In the fifth chapter of this dissertation we will consider deep inelastic scattering off protons. Using the same coherence idea mentioned above, we will find that it is possible to have a simple parton-model interpretation of the approach to scaling observed in lepton scattering off protons. Furthermore, by using the formalism developed before for the deuteron inelastic structure functions and by fitting the experimental data for these same functions, we will be able to perform an extraction of the neutron structure functions, whose properties will be shown to support our general picture for the approach to scaling.

CHAPTER II. NUCLEAR HARD-SCATTERING MODEL

1. Introduction

In this chapter the hard-scattering model for the nuclear case will be presented in detail. Our discussion will be based in the diagram shown in Fig. 1, which represents the inclusive process $A + B \to C + X$. Here the interaction takes place through the emission of virtual sub-systems (a and b), which are the ones that scatter in an internal basic process $a + b \to C + X$, where C is the detected particle. M_0 is the amplitude for this basic interaction, and the amplitudes for the emission of the a and b sub-systems will be contained in distribution functions $G(x, \vec{k}_T)$, to be defined shortly. As was mentioned in the introduction, a and b may be (off-shell) nucleons or composite states that are virtually present in the nucleus, such as deuterons, alpha particles, etc...

It is clear from the diagram that the main ingredient is the impulse approximation. This means that rescattering and shadowing have been neglected, and that we expect the model to work when the effective energy of the internal interaction is large, and for nuclei with a relatively small number of nucleons. Another way of saying this is that multiple scattering will produce small values for the momentum of the detected particle C, due to a loss in momentum in each collision. Thus the model should work best when particle C is not too far away from the edge of phase space.

The internal amplitude M_0 will be taken from experiment, where it is given only on-shell, and extrapolated as indicated below. We could also go one step further, and express M_0 in terms of the even more basic interactions of the constituents of the hadrons. This will not be done because it complicates the model, and also our purpose is to separate these two levels.

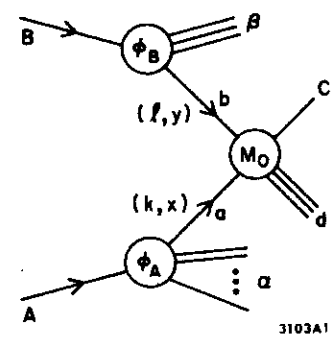

Fig. 1. The basic hard scattering model diagram with the notation used in the text.

We should point out, however, that the various fitted M_0 that we will use are all consistent with the behavior expected in constituent models of hadrons.

We will assume that the detected particle comes from the internal interaction, and this will be true when it has momentum (either longitudinal or transverse) substantially different from the initial beam or target. In our diagram this means that the detected particle does not belong to the multiparticle state $\underline{\alpha}$(or $\underline{\beta}$). This situation could be analyzed in a similar way, however.

We should point out that $\underline{\alpha}$ and $\underline{\beta}$ can have a mass spectrum and do not need to be definite states. This only generalizes the definition of the G function given below. For simplicity, however, we will assume that the energy is such that they are incoherent states with a definite number of nucleons. In other words, the energy is high enough so that the nucleus has broken apart completely, but not too high so that more particles have been created. If the nucleus remains bound, the (1-x) power to be expected in the G function (see Section II-4) should decrease with respect to the one predicted for the unbound case.

Other simplifications will be that in this section we will not distinguish between neutrons and protons, and that spin effects will be neglected. Its inclusion deserves further analysis, because it would allow polarization effects and the spin structure of the short range nuclear force to be studied.

2. <u>The Model</u>

For the analysis of the diagram of Fig. 1, it is convenient to parametrize the different momenta using "infinite momentum frame" variables as follows:

$$A = \left(P_1 + \frac{A^2}{4P_1}\,,\ \vec{0}_T,\ P_1 - \frac{A^2}{4P_1}\right)$$
$$B = \left(P_2 + \frac{B^2}{4P_2}\,,\ \vec{0}_T,\ -P_2 + \frac{B^2}{4P_2}\right) \qquad \text{(II-1)}$$

where a particle's name and four-momentum are denoted by the same symbol except for the off-shell particles a and b. A and B have been defined in a general set of frames along the interaction axis. A specific frame in this set is selected by relating P_1 and P_2. For example, the center-of-mass frame is defined by the conditions

$$P_1 - \frac{A^2}{4P_1} = P_2 - \frac{B^2}{4P_2}$$

and

$$\sqrt{s} = P_1 + \frac{A^2}{4P_1} + P_2 + \frac{B^2}{4P_2} \quad .$$

Also we define the other momenta that are on-shell as

$$\alpha = \left((1-x)P_1 + \frac{\alpha^2 + k_T^2}{4(1-x)P_1}\,,\ -\vec{k}_T,\ (1-x)P_1 - \frac{\alpha^2 + k_T^2}{4(1-x)P_1}\right)$$
$$\beta = \left((1-y)P_2 + \frac{\beta^2 + \ell_T^2}{4(1-y)P_2}\,,\ -\vec{\ell}_T,\ -(1-y)P_2 + \frac{\beta^2 + \ell_T^2}{4(1-y)P_2}\right) \qquad \text{(II-2)}$$

This rather cumbersome set of variables will greatly simplify our later discussion. For example, note that with these parametrizations, the phase space integrals are of the form

$$d^4\alpha = d^2k_T\ \frac{dx}{2|1-x|}\ d\alpha^2 \qquad \text{(II-3)}$$

and then the α^2 integral, due to the corresponding on-mass-shell δ-function, is trivial.

The off-shell momenta are calculated by momentum conservation:

$$a = \left(xP_1 + \frac{k^2+k_T^2}{4xP_1}, \vec{k}_T, xP_1 - \frac{k^2+k_T^2}{4xP_1}\right)$$
$$b = \left(yP_2 + \frac{\ell^2+\ell_T^2}{4yP_2}, \vec{\ell}_T, -yP_2 + \frac{\ell^2+\ell_T^2}{4yP_2}\right) , \qquad \text{(II-4)}$$

where

$$k^2 = \left(x(1-x)A^2 - x\alpha^2 - k_T^2\right)/(1-x)$$
$$\ell^2 = \left(y(1-y)B^2 - y\beta^2 - \ell_T^2\right)/(1-y) \quad . \qquad \text{(II-5)}$$

Note that with these parametrizations,

$$x = \frac{a_0+a_3}{A_0+A_3} \qquad \text{(II-6)}$$

which is the usual light-cone variable. Then x can only have values between zero and one.

Using the Feynman rules, it is a simple matter to evaluate the diagram of Fig. 1. After squaring and integrating over the final state phase space of d and α and β, the inclusive cross section

$$E_C \frac{d\sigma}{d^3C} \equiv R_C$$

achieves the form

$$R_C = \sum_{a,b} \int dx\, d^2k_T\, dy\, d^2\ell_T\, G_{a/A}(x,\vec{k}_T)\, G_{b/B}(y,\vec{\ell}_T)$$
$$r(s',s,x,y) \left[E_C \frac{d\sigma}{d^3C}(a+b \to C+d;s',t',u')\right] \qquad \text{(II-7)}$$

where

$$r = \frac{\lambda(s',k^2,\ell^2)}{xy\lambda(s,A^2,B^2)}$$

and where the x and y integrals run only from zero to one. The variables s', t', u' are those that describe the internal basic process and defined in terms of a, b, and C. The G functions will be defined below. The ratio r of the λ factors is the ratio of the corresponding phase space factors in the cross sections, and

$$\lambda^2[x,y,z] \equiv x^2 + y^2 + z^2 - 2(xy+yz+zx)$$

One finds that throughout the range of variables we are interested in, $r \approx 1$.

A precise definition of the variables will be made later, but the interpretation of the various factors in Eq. (II-7) is clear. The factor $G_{a/A}(x,\vec{k}_T)$ is the probability of finding a constituent of type a in nucleus A with fractional "momentum" x and transverse momenta $\vec{k}_T$. A similar interpretation holds for $G_{b/B}$. The basic cross section factor that actually produces the detected particle C also has a clear probabilistic meaning.

The probability functions are defined as

$$G_{a/A}(x,\vec{k}_T) = \frac{1}{2(2\pi)^3} \frac{x}{(1-x)} |\psi(x,\vec{k}_T)|^2 \qquad \text{(II-8)}$$

where ψ is the bound state Bethe-Salpeter wavefunction with one leg (α) on-shell. It is related to the vertex function ϕ by

$$\psi(x,\vec{k}_T) = \frac{\phi}{k^2-a^2} \quad . \tag{II-9}$$

One can also derive an equation for the electromagnetic form factor of the state A in terms of ψ and the result is

$$F_A(q_T^2) = \sum_a F_a(q^2) \int \frac{dx d^2k_T}{2(2\pi)^3} \frac{x}{(1-x)} \psi^* (x,\vec{k}_T)\, \psi\left(x,\vec{k}_T-(1-x)\vec{q}_T\right) \tag{II-10}$$

where the integral multiplying F_a is the body form factor of the nucleus.

We will see in our analysis that these distribution functions are explicitly measured in the experiments we are considering. For this reason it is important to have a reasonably good knowledge of their properties. In the next sections we will analyze these functions in detail, trying to get information about them from limiting cases, like the nonrelativistic and the short distance behaviors.

3. <u>The Nonrelativistic Limit</u>

We expect our theory to join, when the energies and momenta are small, onto the familiar nonrelativistic treatments. In particular, the G function must be closely related in this limit with the square of the nonrelativistic wavefunction. This requirement will allow us to achieve a clearer understanding of these functions and their expected behavior, and also to explore the way masses should enter into our formalism.

First we want to see the meaning of the x-variable in a nonrelativistic limit. For momenta small with respect to the masses, and in the rest frame of the nucleus, Eq. (II-6) becomes:

$$x \simeq \frac{a}{A} + \frac{k_z}{A} \quad . \tag{II-11}$$

Then x is related to the longitudinal momentum, measuring deviations with respect to a central value $\frac{a}{A}$. Since on the average, and in the rest frame of the nucleus, we expect $k_Z = 0$, this means that on the average $x = \frac{a}{A}$. In other words, each nucleon carries the same fraction of the total momentum of the nucleus. A very reasonable result in the zero binding limit.

Remember also that G is the probability of finding a constituent of A with longitudinal momentum x and transverse momentum $\vec{k}_T$. This means that G must have a maximum at $x \simeq \frac{a}{A}$, the average nucleon longitudinal momentum, and at $\vec{k}_T = 0$. Consider Eq. (II-8), the definition of G, and using equations (II-9) and (II-5), we see that

$$G \sim \frac{\phi^2 x(1-x)}{[k_T^2 + M^2(x)]^2} \quad ,$$

where we have defined

$$M^2(x) \equiv (1-x)(a^2-k^2) - k_T^2 = (1-x)a^2 + x\alpha^2 - x(1-x)A^2 \quad . \tag{II-12}$$

This form implies that G has a maximum at $\vec{k}_T = 0$ and at $x = x_o$, where $M^2(x)$ is a minimum. We find

$$x_o = \frac{A^2 + a^2 - \alpha^2}{2A^2} \cong \frac{a}{A} \tag{II-13}$$

as expected.

In the limit of small momenta one then finds

$$k_T^2 + M^2(x) \cong 2a\varepsilon\left(\frac{A-1}{A}\right) + \vec{k}^2$$

where it has been assumed that the binding energy for nucleon ε is the same for both A and α. The G function becomes

$$G \equiv |\psi_{NR}(\vec{k})|^2 \sim \frac{\phi_{NR}^2(\vec{k})}{[a\varepsilon + \vec{k}^2]^2} \quad ,$$

where

$$\phi_{NR}^2 \sim x_o(1-x_o)\phi^2 \quad .$$

In order to have a better understanding of the function ϕ_{NR}, consider the Schrödinger equation in momentum space

$$\psi_{NR}(\vec{k}) = (a\varepsilon + \vec{k}^2)^{-1} \int d^3p \; V(\vec{k} - \vec{p}) \; \psi_{NR}(\vec{p}) \equiv (a\varepsilon + \vec{k}^2)^{-1} \phi_{NR}(\vec{k}) \quad ,$$

so that the vertex function expresses more or less directly the behavior of the potential V. The falloff of ϕ is related to the softness (or hardness) of the potential. As a simple example consider a general Hulthen model of the nuclear wavefunction:

$$\psi_{NR} = (a\varepsilon + \vec{k}^2)^{-1}(a\varepsilon_1 + \vec{k}^2)^{\frac{1-g}{2}} \quad ,$$

where for the familiar Hulthen deuteron case, one usually chooses g=3, $\varepsilon_1 \sim 36\varepsilon$. The second factor is then much flatter in $\vec{k}^2$ than the first.

A relativistic version of this wavefunction can be achieved by writing

$$\psi = \frac{N(x)}{(k^2 - a^2)} \; \frac{1}{(k_1^2 - a_1^2)^{\frac{g-1}{2}}} \quad , \qquad \text{(II-14)}$$

where N(x) is slowly varying for x near 1, and where

$$(1-x)(a_1^2 - k_1^2) = M^2(x) + \delta^2 + k_T^2 \equiv M_1^2(x) + k_1^2 \quad , \qquad \text{(II-15)}$$

since we want $M_1^2(x)$ to have a minimum at the same place as $M^2(x)$ $(x=x_o)$.

The form factor for this type of wavefunction is easily seen to fall as

$$F^2\left(q_T^2\right) \sim \left(q_T^2\right)^{-g-1}$$

for large q_T^2. Thus the falloff of the form factor and the behavior of G for large k_T^2 are closely related and also we see that the behavior of G for $x \sim 1$ is closely related to the form factor falloff. This latter relation is the Drell-Yan-West relation.[13]

For general x, the relativistic G function can then be written as

$$G(x,\vec{k}_T) = \frac{N^2(x)\; x(1-x)^g}{2(2\pi)^3} \left[M^2(x) + k_T^2\right]^{-2} \left[M_1^2(x) + k_T^2\right]^{1-g} \qquad \text{(II-16)}$$

For $x \sim x_0$, the denominator factors are rapidly varying and as has been discussed, this reduces to a familiar nonrelativistic Hulthen form. For $x \gg x_0$, the numerator factors control the behavior of G, and

$$G(x,\vec{k}_T) \sim (1-x)^g$$

while its large k_T^2 behavior is $\left(k_T^2\right)^{-g-1}$.

In our analysis, the behavior of G for $x \gg x_0$ will be especially important. Note that this is new information not directly contained in the nonrelativistic wavefunction. We shall also discuss quasielastic scattering which explores the G function for $x \sim x_0$ as well. Let us now turn to a discussion of the calculation of the power g in selected theories of the nucleon-nucleon interaction.

4. Counting Rules

In this section, the choice of appropriate wavefunctions will be discussed. This is not a trivial matter since one would like to have wavefunctions that reduce to familiar forms in the nonrelativistic limit but yet

reflect the correct relativistic behavior (for large k_T and for $x \sim 1$) arising from a specific theory of the nucleon-nucleon interaction. Once the wavefunction is given, our main contact with experimental data is through the structure functions $G(x,k_T)$. A helpful tool for expressing the predictions of specific theories is in terms of "counting rules". These allow one to characterize the asymptotic behavior of G in terms of the number of constituents and the basic interactions of the theory.

The procedure here is to extract the leading behavior from the lowest order diagram in perturbation theory. For "soft" theories, one can show that the higher orders either are small compared to the leading term or have the same behavior. Consider the wavefunction (or structure function) diagram given in Fig. 2, where k is the momentum of particle a and is defined by Eq. (II-4). We shall assume scalar particles for simplicity. Note that A now also means the atomic number of particle A.

Theory A

For a renormalizable interaction between the constituents, such as $\lambda\phi^4$ (vector exchange also is in this category), the falloff of the vertex function arises solely from the constituent propagators. One finds

$$\phi \sim \left(k_1^2 - a_1^2\right)^{1-n} \qquad \text{(II-17)}$$

where the masses in k_1 (see Eq. (II-15)) depend on detailed properties of the force. The wavefunction is

$$\psi \sim \left(k^2 - a^2\right)^{-1}\left(k_1^2 - a_1^2\right)^{1-n} \quad . \qquad \text{(II-18)}$$

Comparison with Eq. (II-14) immediately tells us that

$$g = 2A - 3 \qquad \text{(II-19)}$$

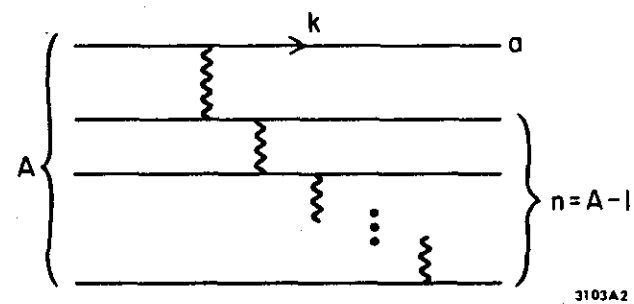

Fig. 2. The wavefunction diagram used to compute the probability functions.

This is the usual dimensional counting prediction for the structure function[14] where one counts nucleons (assumed to be structureless point particles).

Theory B

For a superrenormalizable theory, such as $\phi^2\chi$ (scalar exchange), the vertex function behaves as

$$\phi \sim \left(k_1^2 - a_1^2\right)^{1-n} \left(k_2^2 - a_2^2\right)^{-n} \quad , \qquad \text{(II-20)}$$

where the additional factor arises from the falloff of the gluon propagators. The masses in k_2^2 are to be chosen appropriately. The prediction for g is

$$g = 4A - 5 \quad , \qquad \text{(II-21)}$$

which reflects the increased softness of the potential.

Theory C

As a final and perhaps most relevant example, consider a nucleon-nucleon interaction mediated by the exchange of vector mesons, such as rhos or omegas, with a monopole form factor at each vertex (vector dominance would assume such a behavior to fit the dipole nucleon form factor). One finds

$$\phi \sim \left(k_1^2 - a_1^2\right)^{1-n} \left(k_2^2 - a_2^2\right)^{-2n} \qquad \text{(II-22)}$$

where the masses in the form factors and/or gluon propagators are chosen to be the same for simplicity. The final result is

$$g = 6A - 7 \quad . \qquad \text{(II-23)}$$

This is the same result as found in a $\lambda\phi^4$ theory with a dipole form factor at each four-point vertex, and also is exactly the same result one would get by counting quarks. While one might expect that the quark degrees of freedom become relevant at ultrahigh energies where they can be excited, we see that one gets the same prediction for g in this theory when the nucleon form

factor effects play a role. These, of course, may in turn be due to internal structure, but the internal degrees of freedom need not be fully excited.

For more general structure functions $G_{a/A}$, where the state a is a bound state of a nucleons, a similar analysis can be carried through. One finds in this case

$$g = 2T(A-a) - 1 \qquad \text{(II-24)}$$

where T = 1, 2, or 3, depending upon the theory as discussed earlier. Again, we have assumed full breakup of the nucleus after a is extracted.

Now that it is clear that one can differentiate between theories of the nucleon force by extracting values of g from the data, let us turn to a more detailed discussion of the probability functions.[15] The G's that will be considered here are all of the form (see Eq. (II-16))

$$G_{a/A}(x,\vec{k}_T) = \frac{1}{2(2\pi)^3} \frac{N^2(x)\; x(1-x)^g}{\left[k_T^2 + M^2(x)\right]^2 \left[k_T^2 + M_1^2(x)\right]^{g-1}} \qquad \text{(II-25)}$$

where N(x) is a slowly varying function of x, and

$$M^2(x) = (1-x)a^2 + x\alpha^2 - x(1-x)A^2$$

$$M_1^2(x) = M^2(x) + \delta^2 \; .$$

For large values of A, g is large, and the second term in the denominator controls the falloff in k_T^2. For small k_T^2, G becomes

$$G \propto e^{-R^2 k_T^2}$$

where

$$R^2 \cong \frac{2}{M^2(x)} + \frac{g-1}{M_1^2(x)}$$

For $x \sim x_0$, one expects $R \sim A^{1/3}$, the normal nucleus radius, and hence $M_1^2(x_0) \sim A^{1/3}$. This is then a restriction on the behavior of the parameter δ^2 introduced before. In any case one can fit it directly from the above relation.

The normalization constant of ψ can be computed by the condition

$$\sum_a \int dx\, d^2k_T\, x\, G_{a/A}\,(x,\vec{k}_T) = 1 \quad , \qquad \text{(II-26)}$$

which expresses the fact that the sum of the fractional momenta of the nucleons is the total (fractional) momentum of the nucleus. Note that here we are neglecting the effect of pions that are virtually present in the nucleus, and which are analogous to the "sea" for the parton model of hadrons.

Also it should be noted that the number of particles of type a in the nucleus is given by

$$N^a = \int dx\, d^2k_T\, G_{a/A}(x,\vec{k}_T) \quad , \qquad \text{(II-27)}$$

so that the total number of nucleons is

$$A = \sum_a \int dx\, d^2k_T\, G_{a/A}(x,\vec{k}_T) \quad ,$$

which is consistent with Eq. (II-10), so that $F_A(0) = 1$. In these expressions our approximation of neglecting some effects due to the nonconservation of particle number has been explicitly used.

The function $N^2(x)$ that appears in G will be chosen so that $N^2(x)\, x(1-x)^g$ has a maximum at $x = x_0 = a/A$. This means that

$$N^2(x) = N_0^2\, x^{\alpha-1} \quad , \quad \text{where} \quad \alpha = \frac{g\, x_0}{1-x_0} \quad . \qquad \text{(II-28)}$$

For the case of the deuteron, for example, $g = 5$, so that

$$N(x) = N_0 x^2 \quad .$$

(See Section (IV-1) for a more detailed analysis of the deuteron.)

The general form for G that we have adopted, Eq. (II-25), has several properties that are worth noting:

- G is peaked at $k_T = 0$ and the transverse momentum distribution falls more and more rapidly as A increases.
- G is peaked at $x \sim a/A$. The most likely momentum configuration is that one in which the nucleons share equally the total momentum of the nucleus.
- The power g which controls both $x \sim 1$ and large k_T is very simple to characterize in terms of the basic binding interaction and the number of constituents.
- The shape of G in the nonrelativistic limit does not restrict the behavior for $x \sim 1$ for general models (although they are strongly correlated in our simple models). A measurement of G for $x \sim 1$ is new information that is not accessible to conventional nuclear theory.

CHAPTER III. RELATIVISTIC INTERACTIONS BETWEEN NUCLEI

After having presented the formalism of our model, as a first application we will consider inclusive scattering of nuclei. The next chapter will contain electromagnetic interactions in nuclei.

1. High Energy Limit

In order to get simple predictions that can easily be compared with experiment without extensive numerical calculation, we will first analyze the situation in which the energy per nucleon is large compared to the nucleon mass. The kinematics for this regime is quite simple:

$$\begin{aligned} s' &= xys \\ t' &= yt \\ u' &= xu \\ d^2 &= xys + yt + xu \end{aligned} \qquad \text{(III-1)}$$

and

$$C_T^2 = \frac{ut}{s} = C_T'^2$$

The condition $d^2 > 0$ restricts the range of x and y that contribute for fixed values of s, t, u.

Note that the internal reaction can be inclusive ($d^2 > 0$) or exclusive ($d^2 = 0$). This last situation is the case in quasielastic scattering, for example.

All inclusive basic processes of interest to us here will be parametrized as

$$\left[E_C \frac{d\sigma}{d^3C}\right]' = E(s') \left(1 - |x_F'|\right)^H f(k_T') \qquad \text{(III-2)}$$

and exclusive processes as

$$\left[E_C \frac{d\sigma}{d^3C}\right]' = E(s')\delta\left[(k+\ell-C)^2 - d^2\right] f(k_T') \quad , \qquad \text{(III-3)}$$

where $k_T' = C_T - k_T - \ell_T$ and $E(s')$ is assumed rather slowly varying. H will be assumed to be constant, but a dependence on transverse momentum can easily be included. The function $f(k_T')$ is strongly peaked for $k_T' = 0$ (for small k_T' it could be written as an exponential $e^{-r^2 k_T'^2}$, for example).

Now we will go into a discussion of our model in some regions of phase space in which it is easy to get predictions.

First define (m is the missing mass)

$$\varepsilon = \frac{m^2}{s} = 1 - x_R \cong 1 - \frac{|\vec{C}_{cm}|}{|\vec{C}_{max}|}$$

$$x_T = \frac{C_T}{C_{max}} \qquad x_R = \sqrt{x_T^2 + x_L^2} \qquad \text{(III-3)}$$

$$x_L = \frac{C_L}{C_{max}} \cong \frac{t-u}{s} \quad ,$$

and for the most part we will concentrate in the region ε close to zero.

A. Projectile fragmentation region

When t is fixed (and s,u large), one finds ($x_R = x_F$, Feynman's variable)

$$1 - x_F = 1 + \frac{t+u}{s}$$

and

$$1 - x_F' = 1 + \frac{yt + xu}{xys} \quad , \qquad \text{(III-4)}$$

and hence $x_F' \cong x_F/y$. The condition $d^2 > 0$ becomes $y > x_F$. In this regime formula (II-7) becomes

$$R_C \sim \sum_{ab} \int_0^1 dx d^2k_T \; G_{a/A}(x,\vec{k}_T) \int_{x_F}^1 dy d^2\ell_T \; G_{b/B}(y,\vec{\ell}_T) \left[E_C \frac{d\sigma}{d^3C}\right]' \quad . \qquad \text{(III-5)}$$

A1. First consider an inclusive basic process. Since $f(\vec{k}_T')$ in formula (III-2) is strongly peaked in $k_T'^2$, we can approximate the k_T and ℓ_T integrals by replacing k_T^2 and ℓ_T^2 in the G's by the mean value K^2 which should be of the order of C_T^2. The inclusive cross section is the proportional to

$$R \propto \int_{x_F}^1 dy \; \frac{N^2(y)\; y(1-y)^{g_B}}{\left[K^2+M^2(y)\right]^2 \left[K^2+M_1^2(y)\right]^{g-1}} \; (1-x_F/y)^H \quad . \qquad \text{(III-6)}$$

Note that the distribution for the target $G_{a/A}$ has integrated out in this limit, and that R depends on A through its normalization only.

If $C_T^2 \gtrsim M_1^2(x_0)$, and if x_F is not small compared to x_0, then the main variation in the integrand is from the factors of $(1-y)$ and $(1-x_F/y)$. The first factor cuts off the integrand near $y = 1$ and the other near $y = x_F$. If only their variation is retained, and the denominators taken constant, we have

$$R \propto \int_{x_F}^1 dy (1-y)^{g_B} (1-x_F/y)^H$$

$$R \sim (1-x_F)^{g_B+H+1} \qquad \text{(III-7)}$$

A more accurate treatment is possible but the above will suffice for our purposes. In the target fragmentation region, where u is fixed and s,t large, the above arguments can be repeated with the result that

$$R \sim (1+x_F)^{g_A+H+1} \quad , \qquad \text{(III-8)}$$

where g_A is the power behavior of the target distribution function $G_{a/A}$. This result could also have been achieved by simply interchanging the target and beam particles in the previous result. These predictions will be compared to data in a later section.

One can estimate the range of validity in x_F of the above formulas by a simple argument. The momentum fraction x_F must be large enough so that the particle is out of the "quasielastic" peak where the denominator factors in Eq. (III-6) are rapidly varying. The average momentum fraction x_B of particle B is $\langle x_B \rangle = 1/B$. The average x retained by the detected particle of Eq. (III-2) is roughly $\approx 1/(H+2)$. Therefore, the behavior given by Eq. (III-7) should hold reasonably well for $x_F \gtrsim 1/B(H+2)$. For example, for the process deuterons $\to \pi^-$, this limit is $x_F \gtrsim 1/2x5 = 1/10$, and most of the x_F range is covered.

A2. For an exclusive basic process, which yields a familiar quasielastic reaction, the calculation is also quite simple. Using Eq. (III-3) and expanding the arguments of the delta function for the case $b + n \to C + n$, where b and C are nucleons, one finds that a reasonable approximation is:

$$\left[E \frac{d\sigma}{d^3C}\right]' = E(s')\delta\left[x(s-A^2-B^2)(x_F-\Delta-y)\right] f(k_T')$$

where the shift Δ has to be calculated using more exact kinematics. At high energies $\Delta \to 0$.

Again the x integral is not restricted and the full inclusive cross section is

$$R \propto G_{C/B}\left(x_F-\Delta, K^2\right)\left(\frac{d\sigma}{dt}\right)' \qquad \text{(III-9)}$$

The quasielastic peak should occur at $x_F = C/B + \Delta$. This is slightly larger than the naive expectation C/B, the most likely momentum in the state B. This shift will be included in all our numerical calculations. Equation (III-9) can be interpreted as a relativistic generalization of the Glauber approximation but with a more precise definition of the covariant wavefunction.

Although for simplicity we have discussed in detail the kinematics of the high energy region only, it can be shown that our results should be quite accurate at lower energies. For example, one important conclusion of our analysis was that the lower limit of the y-integral is equal to x_F. This comes from the condition $(k+\ell-C)^2 > d^2$. We have calculated this equation more exactly, assuming small transverse momenta and $\langle x \rangle = d/A$, and found that the corrections are small for the range of energies of the experiments we want to analyze here (kinetic energies per nucleon ≈ 1 or 2 GeV). At the quasielastic peak, for example, we find

$$\begin{aligned} \Delta &= .07 \quad (dC \to pX) \\ \Delta &= .05 \quad (CC \to pX) \\ \Delta &= .075 \quad (CC \to HeX) \end{aligned} \qquad \text{(III-10)}$$

and these shifts show clearly in the experimental data (see Figs. 7 and 8). The values were calculated assuming a specific internal process. For example, in the case $CC \to HeX$, the internal process was $Hep \to HeX$. Another possibility could have been $He + He \to He + X$, but this gives a shift at the quasielastic peak that does not agree with the experimental data. The approximate naive position of the quasielastic peak (b/B) is determined by the nature of the fragment b arising from the beam. The kinematical shift Δ then determines the fragment, a, arising from the target. Additional subsidiary peaks or shoulders in the data could be due to more than one basic process being

important. These can be identified using the above procedure even if the dominant ones change with angle.

B. Large p_T region

Another situation in which we can get simple predictions from the model is when the produced particle (C) has large transverse momentum (s,t,u large, and masses negligible). In this regime ($\theta_{cm} \cong 90°$), we have that

$$x_L \cong 0$$

$$x_R \cong x_T$$

and

$$1 - x_R' \cong \frac{d^2}{s'} = \frac{x_T}{2}\left(\frac{1}{x} + \frac{1}{y}\right) \quad . \qquad \text{(III-11)}$$

B1. Inclusive basic process. The condition $d^2 > 0$ means that in the limit of primary interest to us x and y in formula (II-7) are going to be both close to one. By a similar analysis as in section A, the $\vec{k}_T$ and $\vec{\ell}_T$ can then be integrated out and we can write approximately ($G(x) \sim (1-x)^g$)

$$R_C \sim \int_0^1 dx \int_0^1 dy (1-x)^{g_a} (1-y)^{g_b} \left[R_C'(a+b \to C+X)\right] \theta(d^2) \quad , \qquad \text{(III-12)}$$

which can be applied, for example, to pion and proton (not including the quasielastic peak) production at large transverse momentum.

We will consider two different parametrizations for the internal cross section:

$$\text{(a)} \quad R_C' \sim (1-x_R')^H f(C_T'^2) s'^P \qquad \text{(III-13)}$$

and then one finds, using Eq. (III-12):

$$R_C \sim \varepsilon^{F+H+1} (C_T^2)^P f(C_T^2) \quad , \qquad \text{(III-14)}$$

where $F = 1 + g_a + g_b$ and where ε is close to zero. For ε not near zero, there is a function which is slowly varying in ε that multiplies this result.

We see that this regime gives us information about the distribution functions of both target and projectile. It also follows that the C_T^2 dependence is the same for the complete process as it is for the internal interaction, except for the $(C_T^2)^p$ factor.

(b) Assume the form

$$R_C' \sim (1-x_R')^H \frac{1}{(-t')^T(-u')^T(s')^{N-2T}} \quad , \qquad \text{(III-15)}$$

which can be written as

$$R_C' \sim (1-x_R')^H \frac{1}{(C_T^2)^N} \left(\frac{x_T^2}{4xy}\right)^{N-T} \quad .$$

Inserting this expression into Eq. (III-12), we get

$$R_C \sim \varepsilon^{F+H+1} \frac{1}{(C_T^2)^N} \quad .$$

It is then clear that this is just a special case of Eq. (III-14) with $f(C_T^2) = 1/(C_T^2)^{N+p}$.

B2. Exclusive basic process. In some cases (quasielastic scattering), the internal basic process is going to be dominated by elastic scattering. This means that the cross section can be written as $(G(x) \sim (1-x)^g)$

$$R_C \sim \int_0^1 dx \int_0^1 dy \; (1-x)^{g_a}(1-x)^{g_b} \left[R_C'(C + b \to C + d)\right] \quad , \qquad \text{(III-16)}$$

where $R_C' = \delta(d^2) \frac{s'}{\pi} \frac{d\sigma}{dt} (C + b \to C + d)$ and R_C' now contains a factor $\delta(d^2)$.

As before, we consider two possible parametrizations for the internal interaction:

(a) $\frac{d\sigma}{dt} \sim s'^p f(C_T^2)$

which gives the prediction

$$R_C = I(\varepsilon)\; \varepsilon^F (C_T^2)^p f(C_T^2) \quad . \qquad \text{(III-17)}$$

Note that in this case the multiplying function $I(\varepsilon)$ is going to be rapidly varying, in order to reproduce the quasielastic peak. Right at the quasielastic peak we have $\langle y\rangle \simeq 1/B$, $\langle x\rangle \simeq 1/A$, where A and B are the atomic number of the states A and B respectively. Using $d^2 = 0$, we get for the peak value (neglecting kinematic mass effects)

$$\varepsilon_Q \simeq 1 - \frac{2}{A+B} \quad .$$

One expects that $I(\varepsilon)\; \varepsilon^F$ will be rapidly varying and will lead to a quasielastic peak for $\varepsilon \sim \varepsilon_Q$. For $\varepsilon > \varepsilon_Q$, $I(\varepsilon)$ should vary much less, and the main ε dependence should come from the ε^F factor.

This result can be formally connected with the one obtained in Section B1 for inclusive $(N + N \to N + X)$ internal scattering by taking the limit $H \simeq -1$ in this latter case. The data for $(N + N \to N + X)$ seems to have a large inelastic component with $H \sim -1$ which contributes a term to R_C with the same ε power as an elastic basic scattering process. The elastic processes should have a quasielastic peak whereas the inelastic will not, in general.

(b) Consider now the parametrization

$$\frac{d\sigma}{dt} \sim \frac{1}{(-t')^T(-u')^T(s')^{N-2T}}$$

which gives the result

$$R_C = \frac{I(\varepsilon)\ \varepsilon^F}{(C_T^2)^N}$$

in the same general form as before but with a power law dependence on transverse momentum.

The results given above can be generalized with the inclusion of mass effects. We expect, for example,

$$R_C = I(\varepsilon)\varepsilon^{F+1+H} J(C_T^2) \qquad \text{(III-18)}$$

where $F = 1 + g_a + g_b$ as before and $I(\varepsilon)$ is a slowly varying function of ε for $\varepsilon \to 0$ (but rapidly varying around the quasielastic peak). $J(C_T^2)$ is determined by the fit to the basic reaction using model a or is $(p_T^2 + M_e^2)^{-N}$ for model b where M_e is some effective mass. ε also contains mass effects because it must have the correct threshold behavior and its general definition is

$$\varepsilon = 1 - \frac{|\vec{C}_{cm}|}{|\vec{C}_{cm}|_{max}} \quad . \qquad \text{(III-19)}$$

The fit to the data has to be made at different energies, with $|\vec{C}_T|$ fixed, in order that the ε dependence can be extracted. For the $|\vec{C}_T|$ dependence, we need data for fixed ε (all data at $\theta_{cm} \simeq 90°$).

C. Summary

In the previous sections we have presented a detailed analysis of our relativistic model and the predictions it gives when applied in specific regions of phase space (projectile fragmentation, target fragmentation and large p_T). While because of their simplicity we have considered only these special cases, it is possible to obtain a generalization of these results that is valid for all angles. In fact, using Eq. (III-12) it can be shown

that when ε is close to zero,

$$R_C = I(\varepsilon)\ \varepsilon^{F+1+H}\ (1-x_R z)^{-F_-}\ (1+x_R z)^{-F_+}\ J(C_T^2) \quad , \qquad \text{(III-20)}$$

where $z = \cos\theta_{cm}$, $F_- = 1 + g_a$, $F_+ = 1 + g_b$. As before $F = 1 + g_a + g_b$, and $I(\varepsilon)$ is a slowly varying function of ε. This result is valid for an inclusive internal process parametrized in the form

$$R_C' \sim (1-x_R')^H\ J(C_T'^2) \quad . \qquad \text{(III-21)}$$

Although Eq. (III-20) was derived assuming $|z|$ not near one (outside the forward and backward cones), we see that it also has the correct limit inside those regions. This expression can then be used to characterize the inclusive nuclear reaction at all angles. Furthermore, since we expect a smooth transition from the regions of validity of Eq. (III-20) to other regions of the Peyrou plot (central region), this equation can be used to fit the data everywhere (with effective powers).

2. Pion Production

As the first application of the model, we shall consider π^- production in the projectile fragmentation region for several different reactions. The data in Fig. 3, taken from J. Papp et al.,[2] clearly supports a prediction of the model that the cross section does not depend upon the target except for an overall factor (which goes as $A^{1/3}$ due to the circumferential nature of the scattering) except very near threshold.

A proper treatment of these kinematic effects is necessary in certain kinematic regions. For example, one expects that in the fragmentation region of processes such as $p + A \to \pi^- + X$, the cross section will be the same as for $p + p \to \pi^- + X$. This is not so at the lower energies because of a kinematic effect that is essentially the same for all targets ($A \geq 2$) and which changes

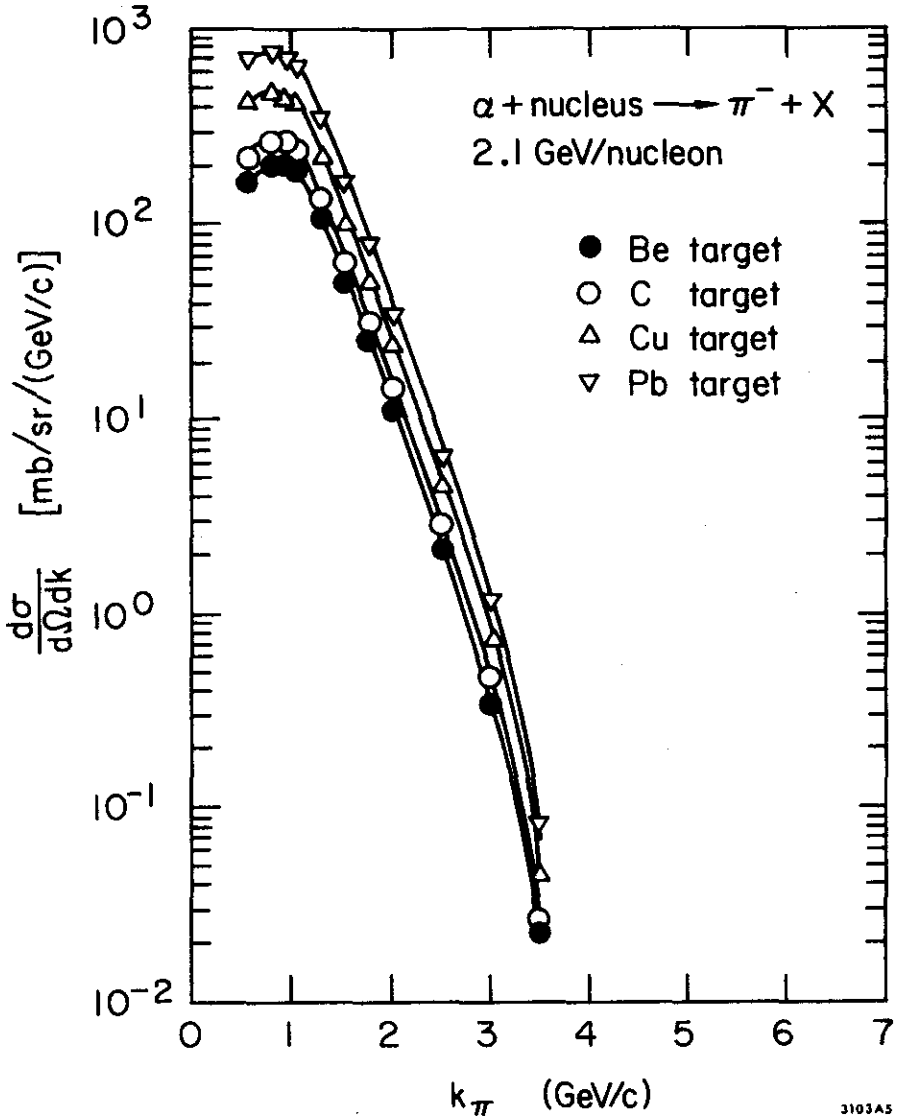

Fig. 3. Scattering from selected targets according to Ref. 2 to illustrate A independence of the shape of the x spectrum.

the shape of the cross section. The point is that near threshold, the integration over x (the target longitudinal momentum variable) does not go from zero to one and actually the allowed interval shrinks to a point for $x_F \to 1$. Now k^2 is negative for most values of x, and for $x_F \sim 1$ some of the energy for the reaction must be extracted from the Fermi motion in the target.

The basic reaction $p + p \to \pi^- + X$ will be parametrized as

$$R' = R_0(1-x_F') \, e^{-4x'_F} \, e^{-15k'^2_T} \quad . \qquad \text{(III-22)}$$

This is a reasonable representation to the data of Akerlof et al.[16] and E. Gellert.[17] We will treat neutrons and protons the same in order to keep the treatment simple.

$pC \to \pi^-$: Using the R' given above, and calculating numerically using exact kinematics, we get the result shown in Fig. 4. We have not computed the normalization (this would require a careful treatment of absorption) and have normalized our calculation to the data.[2] For energies in the range of interest, one finds that R scales (for different energies) and for fixed (small) t, that

$$R \propto (1-x_F)^3 \quad , \qquad \text{(III-23)}$$

which is not very different from Eq. (III-22) except near $x_F = 1$. Note that a change in the power by 1 is a factor of two difference at $x_F = 0.6$ if normalized at $x_F = 0.2$. This form does not depend upon the specific target distribution function and hence is the same for all the different counting rules. The properties of the target wavefunction do not enter except in the overall normalization constant.

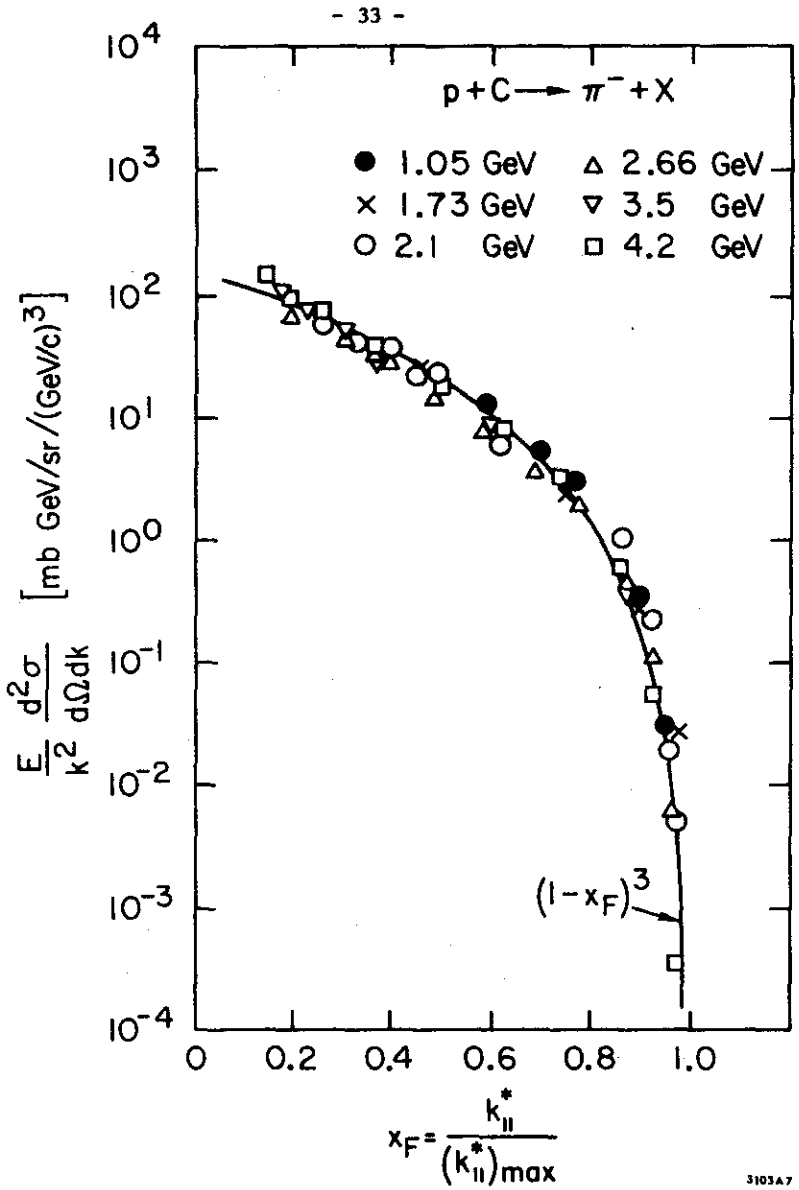

Fig. 4. The x_F spectrum compared to the carbon data illustrating scaling.

For backward scattering, i.e., u-fixed, the result depends strongly on the theory of the target wavefunction. We find (A = 12)

$$R \sim (1+x_F)^b$$

where b = 23, 45, 67 for the three possible theories (A, B, C, respectively) of the previous section.

<u>DC → π⁻</u>: From the analysis of the previous section, we know that H = 3. The prediction for R should now depend upon the deuteron wavefunction. For t-fixed, we find

$$R \sim (1-x_F)^f \qquad \text{(III-24)}$$

where f = 5, 7, and 9 for the three theories. If we compare with experiment,[2] Fig. 5, the value 9 is clearly favored. Recall that this is the theory of vector meson exchange (omegas or rhos) with monopole form factors. These counting rules are the same as quark counting, i.e., T = 3.

For backward scattering, u-fixed, one finds

$$R \sim (1+x_F)^b$$

where b = 25, 47, 69 for the respective theories.

<u>HeC → π⁻</u>: This reaction clearly shows, see Fig. 6, the effects of strong correlation in the initial wavefunction since pions are observed with <u>one-half</u> of the incident alpha particle momentum. The predictions are

$$R \sim (1-x_F)^f \qquad \text{(III-25)}$$

where f = 9, 15, and 21. The data[2] of Fig. 4 shows that f is definitely between 17 and 25, and 21 is a good fit. This data again favors model C, T = 3.

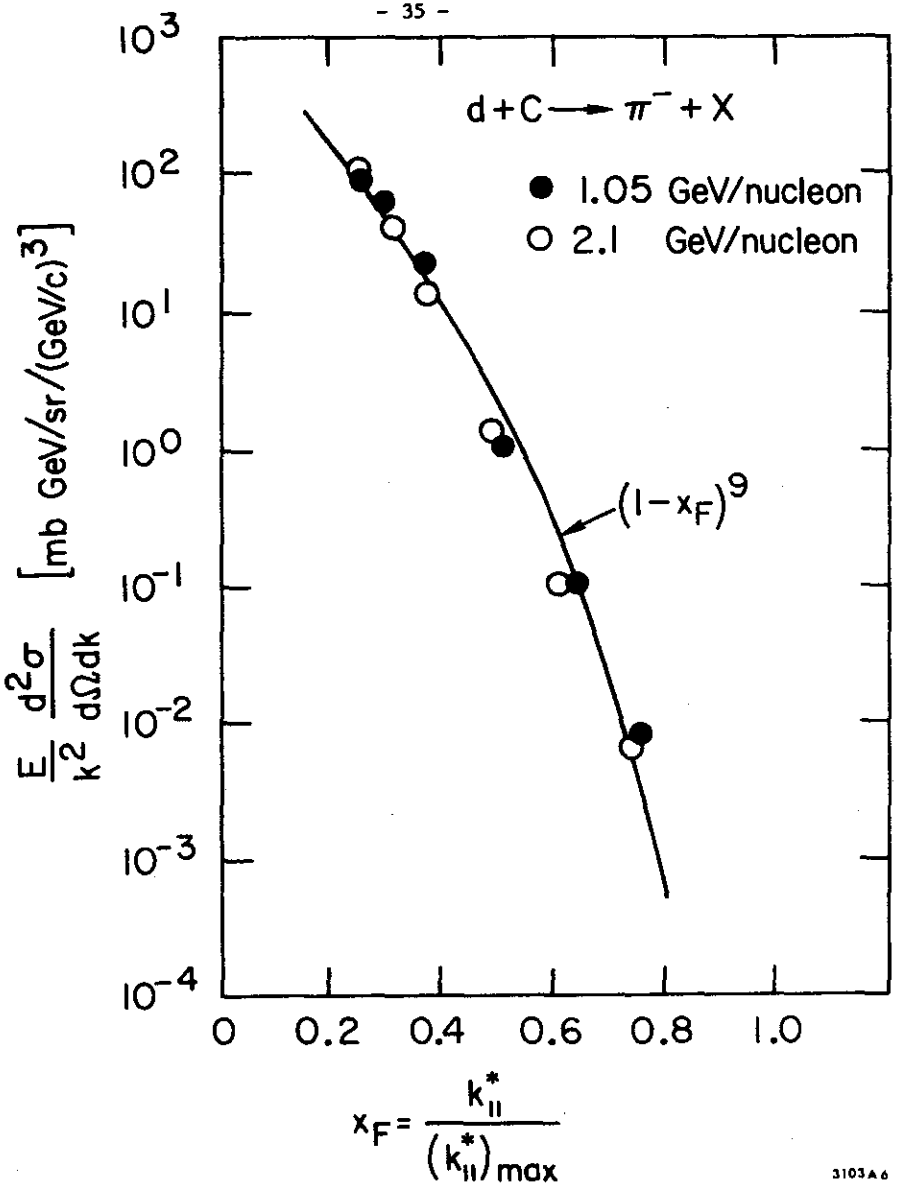

Fig. 5. The prediction for T=3 compared to the data of Ref. 2 for a deuteron beam.

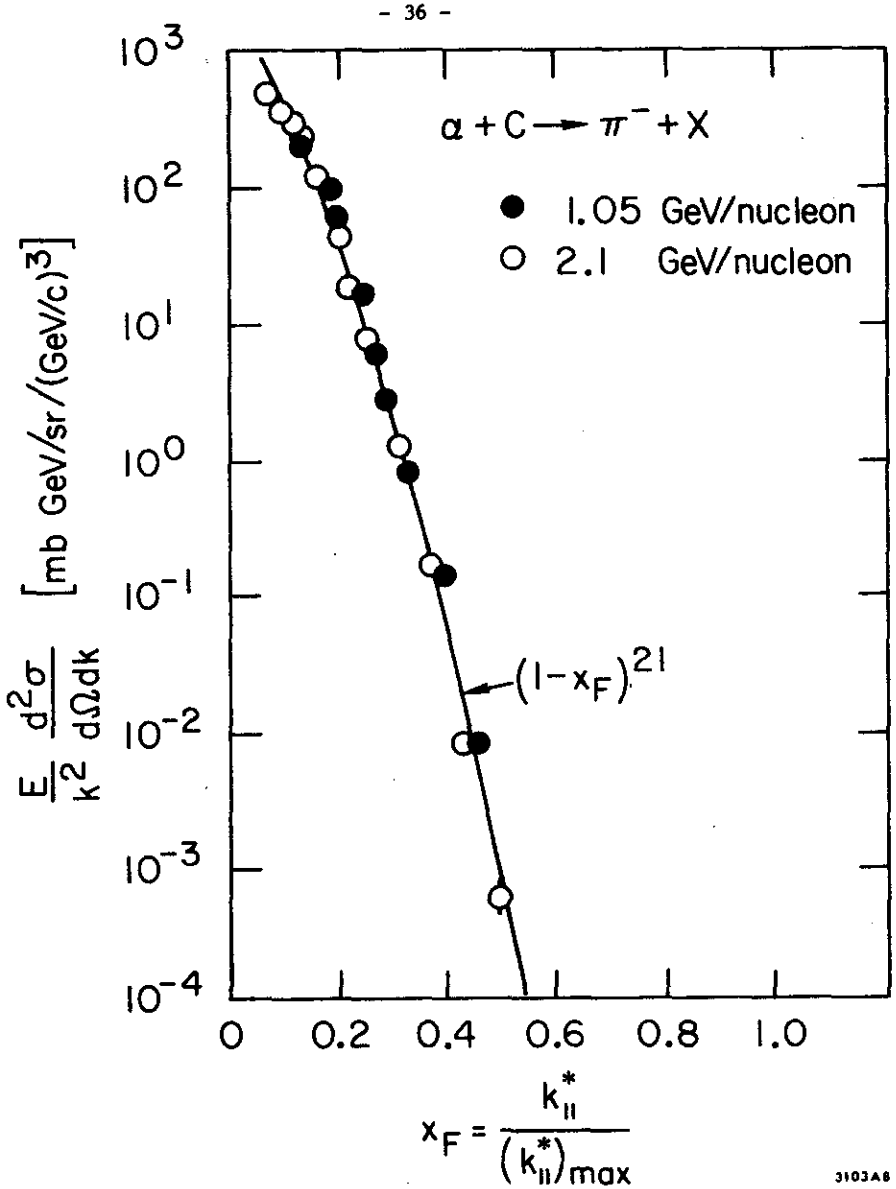

Fig. 6. The prediction for T=3 compared to the data of Ref. 2 for an alpha particle beam.

In the backward direction, we find

$$R \sim (1+x_F)^b$$

where b = 25, 47, and 69.

We have also compared our predictions for forward scattering from beryllium and the agreement with the data of Ref. 4 is quite satisfactory.

3. Proton Production

Now let us consider inclusive proton production. First, some examples will be discussed outside the quasielastic peak, that is, $x_F > 1/B$. Then quasielastic scattering will be treated. As we have stressed before, this is a test of the wavefunction in the relativistic regime, whereas the quasielastic peak depends upon the most likely nucleon configuration which can be adequately described by a nonrelativistic wavefunction.

As explained before, the effective internal cross section should include some kinematical effects arising from the target due to the low energy but this will be neglected here. From pp → pX data, we conclude that $H_{eff} \simeq -1$ (recall Eqs. (III-2) and (III-3)).

DC → P: For this case, the prediction follows just as in the pion case and one finds in the forward direction

$$R \sim (1-x_F)^f \qquad \text{(III-26)}$$

where f = 1, 3, or 5 for the three theories. The data does not extend very far above the quasielastic peak. In Fig. 7 the prediction for f = 5 is graphed. The data[3] seems to indicate that f is between 4 and 5. This is again consistent with theory C. The full curve in Fig. 7 will be discussed shortly.

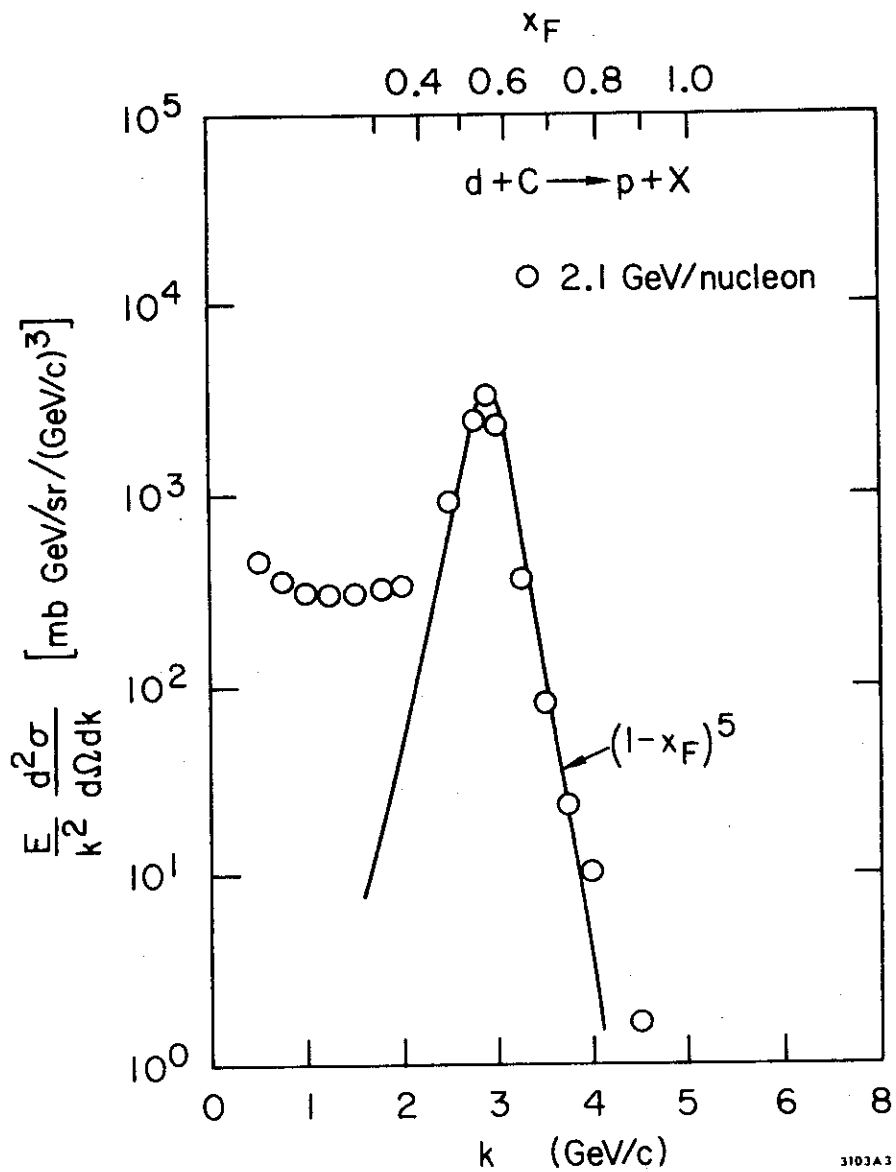

Fig. 7. The prediction for inclusive protons from a deuteron beam for T=3. The full curve is a fit to the quasielastic peak using the theory in the text. The curve asymptotes to $(1-x_F)^5$ but is steeper near the quasielastic peak as discussed in the text.

For backward scattering, the prediction is

$$R \sim (1+x_F)^b$$

where b = 21, 43 and 65.

CC → P: Just to see how far our model can be pushed, consider this reaction. Obviously, the predicted powers are going to be very large but nevertheless are susceptible to analysis. The consistency of this model can at least be tested and its trend as the nucleon number increases. In this case, the forward and backward predictions are the same and one finds

$$R \sim (1 - |x_F|)^f \qquad \text{(III-27)}$$

where f = 21, 43, or 65. The data from Ref. 3 in Fig. 8 seems to indicate a large value of f, with 65 being a quite acceptable fit, but more data is needed for a definitive test.

CC → He4: The predictions for f are 15, 31, or 47 if the intermediate state b is an alpha particle. In Fig. 8 the curve for f = 47 is consistent with the data.[3] The other possibilities are nowhere near the experimental curve.

Quasielastic: We have computed quasielastic scattering for one sample process, DC → pX. The deuteron wavefunction was chosen from model C, so that g = 5 and in order to get a reasonable rms radius, δ^2 = 200 ae. Setting $k^2 = \vec{C}_T^2$ in Eq. (III-9), one gets the curve shown in Fig. 7. The agreement is quite good throughout the peak region and above. The excess rate at low x_F must be due to multiple scattering in the nucleus which we have made no attempt to calculate.

We have compared predictions of the above type for beryllium target data[4] and the fit is satisfactory.

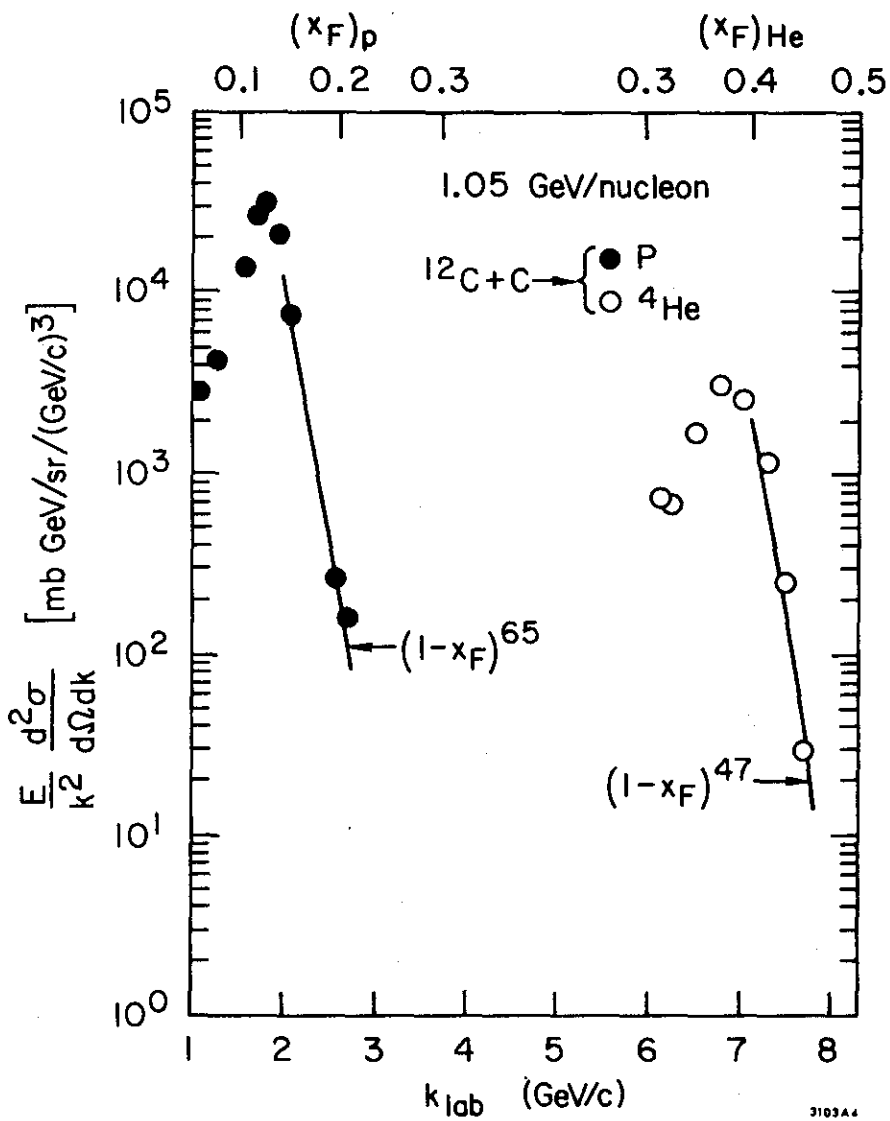

Fig. 8. Two inclusive processes for a carbon beam illustrating the counting rules and the positions of the quasielastic peaks.

4. Conclusions

The model we have presented here is quite general and can be applied to many different types of reactions. In this chapter we have analyzed the case of strong interactions, and in the next one we will consider electromagnetic interactions in nuclei. Weak interactions can be treated in a similar way.

We must point out that in order to compare our simple predictions with experimental data, this has to be done for x_F away from quasielastic peaks (near one), and at high energies per nucleon. This last point is worth commenting on a little more. The energy has to be high for two reasons, first so that masses can be neglected, and second so that we are sure that the nuclei in the reaction have broken apart, without leaving any nuclear bound states. A generalization that includes this last situation should not be difficult, however. Also note that the incident energy per nucleon is not a good measure for "high" energy if we are, for example, in the target fragmentation region. Then it is better to consider some invariant quantity, like the center of mass energy.

The effects of absorption were completely neglected in the present treatment, and this is a very important omission that must be remedied if one wishes to compute the absolute normalization of the reactions discussed here.

In conclusion, we feel that the general approach used here to describe the high energy scattering of heavy ions has many advantages over the conventional approach using Schrödinger wavefunctions and standard scattering theory. Some aspects of our model that are worth mentioning are:

(1) We have presented a fully relativistic formulation of the scattering of bound states. The formalism has a very simple physical interpretation. The relativistic wavefunctions are shown to be simply related to familiar nonrelativistic choices. The relativistic situation is described in terms of distribution functions $G(x,\vec{k}_T)$, which can be explicitly measured, and which have a simple probabilistic interpretation.

(2) We have developed counting rules that allow one to predict in a simple way the general behavior of the reaction cross sections. These counting rules are expressed in terms of the basic short range behavior of the nucleon-nucleon force.

(3) Good agreement with several experiments is attained for one simple model. This model has as its basic force the exchange of vector mesons with monopole form factors at each vertex. The agreement with experiment holds for both meson production and proton inclusive processes. Once the force is given, there are <u>no</u> parameters (except for normalization) outside the quasielastic peak, and even this needs δ^2 only. It is important to add that we have checked several other reactions not included here, and all are consistent with the prediction of the counting rules for the same simple model.

(4) The force model that fits experiment is shown to have the same counting rules as the quark-dimensional counting model discussed by Brodsky and Chertok.[18] Since the reactions discussed here are certainly at too low an energy to fully excite the quark degrees of freedom, the agreement between the quark model and the elastic deuteron data can perhaps be more easily understood in terms of our model. Evidently, the theory is much smoother than one would expect <u>a priori</u> in its connection between very high energies (excitation of quark degrees of freedom) and the range of energies we have discussed here.

This connection does not continue, however, when we consider reactions like elastic pp scattering, in the region where $s \to \infty$, $\frac{t}{s}$ fixed. Our force model gives $d\sigma/dt \sim \frac{1}{s^6} f(\frac{t}{s})$, which differs significantly from the quark dimensional counting prediction $\frac{1}{s^{10}} f(\frac{t}{s})$. The latter result agrees with the data at very high energies, while the former does the same in the range of energies we are considering here.

(5) Our results for the forward and backward directions scale in the sense of being a function only of x_F, independent of the energy. This is clearly shown in the data. It is interesting to note that this is true even when all the effects of masses are included, as we checked explicitly by computing the cross section for the case $(p + C \to \pi^- + X)$ numerically. For the large p_T region, this scaling means that the cross sections are functions of x_F and p_T only.

(6) The model used here provides a simple yet relativistic description of quasielastic scattering. It contains the standard Glauber theory and the standard impulse approximation in the low energy limit.

(7) Predictions are easily made and are given for as yet unmeasured processes which can serve as a more severe test of our model. Large p_T reactions were analyzed in detail, and results given for backward scattering. Furthermore, a general expression that is valid for all angles was presented.

(8) The model allows one to simply describe a region of the wavefunction that cannot be described sensibly in the nonrelativistic approach. The experimental data is thus exploring a new regime of nuclear physics and providing new tests of nuclear theory.

CHAPTER IV. ELECTROMAGNETIC INTERACTIONS IN NUCLEI

The analysis of the previous chapter showed that our relativistic model gave good results when applied to collisions between nuclei, and that the data under consideration explores new aspects of the nuclear wavefunction which have a very simple interpretation in terms of the basic interactions between nucleons in the nucleus. A similar regime can be explored with electromagnetic probes. In this chapter we will consider this situation, in particular electromagnetic nuclear form factors at large transfer momentum and deep inelastic scattering off light nuclei. For the most part we will concentrate on the deuteron.

1. Nuclear Electromagnetic Form Factors

As we saw in Section (II-2), for scalar nucleons we can write the form factor at four-momentum transfer q^2 $(= -q_T^2)$ in terms of the nuclear wavefunction with one particle on-shell $\psi_a(x,\vec{k}_T)$ as

$$F_A(q^2) = \sum_a F_a(q^2) \int \frac{dx\, d^2k_T}{2(2\pi)^3} \frac{x}{(1-x)} \psi_a^*(x,\vec{k}_T+(1-x)\vec{q}_T)\, \psi_a(x,\vec{k}_T) \quad , \qquad \text{(IV-1)}$$

where the sum runs over the nucleons (protons and neutrons) in the nucleus A. $F_a(q^2)$ has been replaced by its on-shell value, and the integral multiplying it is then the intrinsic body form factor of the nucleus.

A very plausible wavefunction ψ, which we saw before gives a G function (see Eq. (II-16)) with several correct properties, is

$$\psi(x,\vec{k}_T) = \frac{N(x)(1-x)^{\frac{g+1}{2}}}{\left[k_T^2 + M^2(x)\right]\left[k_T^2 + M^2(x) + \delta^2\right]^{\frac{g-1}{2}}} \qquad \text{(IV-2)}$$

where for the case of the deuteron $g = 5$ for theory C of Section (II-4) (exchange of vector mesons with monopole form factors at each vertex). We

showed before that this theory gave good results for inclusive reactions, and that this form for ψ was quite successful in reproducing quasielastic scattering data involving the deuteron.

Since for the most part this chapter will be devoted to the deuteron case, let us analyze the G function for this situation. First, since ψ describes one off-shell and one on-shell particle, neither ψ nor G are necessarily symmetric around $x = 1/2$. Isospin symmetry implies that $G_{p/D}(x) = G_{n/D}(x)$, not that $G_{p/D}(x) = G_{n/D}(1-x)$. However, this is a good approximation at not too high energies, when we consider a deuteron as composed of only one proton and one neutron, which means (see Eq. (II-27))

$$\int dx\, d^2 k_T\, G_{a/D}\,(x,\vec{k}_T) = 1 \quad . \tag{IV-3}$$

Note that then this is equivalent to the momentum normalization condition (Eq. (II-26)). The symmetry of G around $x = 1/2$ fixes the function $N(x) = N_0 x^2$.

The deuteron form factor can now be computed from $\psi(x,k_T)$. A fit that can be achieved for our spinless model is given in Fig. 9 for the value

$$\delta_D^2 \simeq 200\ M\ \varepsilon \quad , \tag{IV-4}$$

where M is the nucleon mass and ε is the binding energy of the deuteron. Here the isoscalar form factor was taken to be equal to the proton form factor. Note that this is the same δ_D^2 value that was used before in the analysis of quasielastic scattering (Section (III-3)). The data is from Ref. 19. If spin were put into the model, and especially if D-state effects were then included, the fit could be made much better since the quadrupole contribution naturally gives a shape that is similar to that of the data points.[20] The

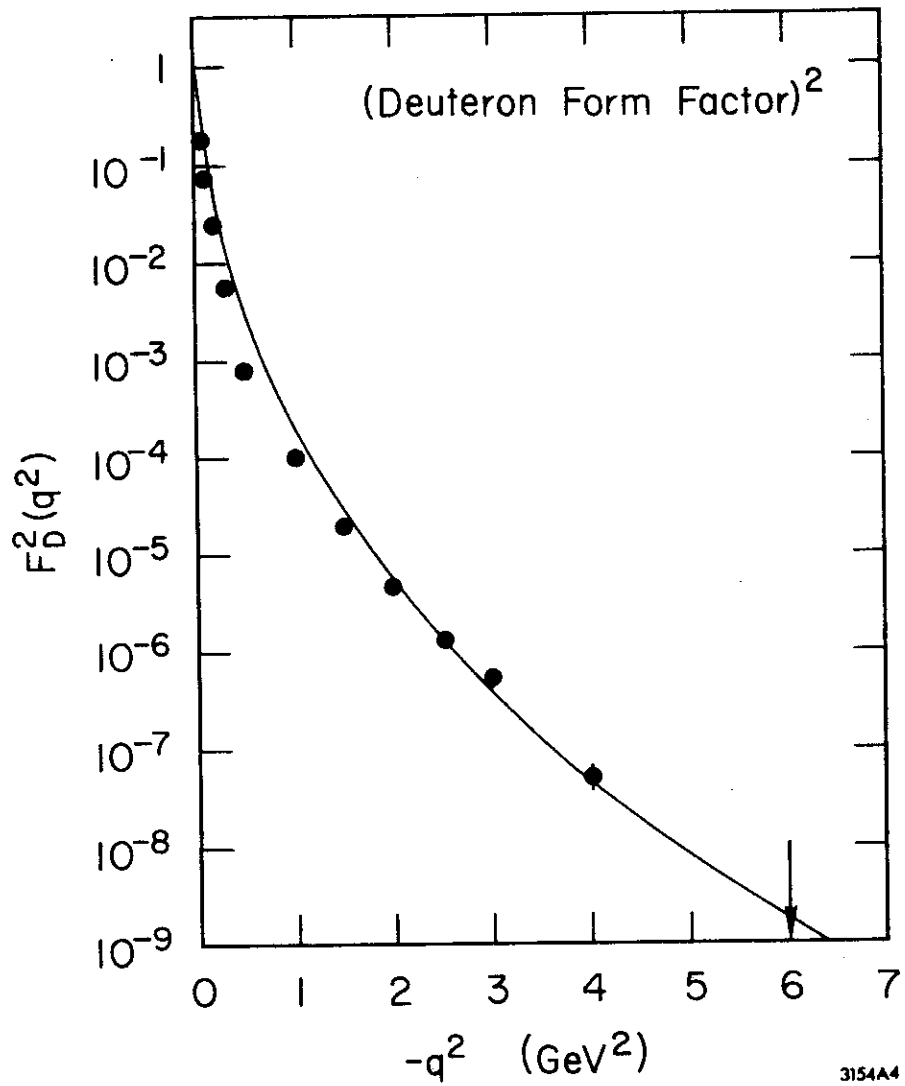

Fig. 9. Fit to the (deuteron form factor)^2.

form factor has, with $g = 5$, the asymptotic behavior in q^2 given by quark counting.[21]

As was mentioned before (see Section (III-4)), our force model predicts, when applied to elastic processes like $pp \to pp$, a behavior with s that is different from the result obtained using quark dimensional counting rules. This means that at high energies our force model has to change, providing a factor of the form $1/(1-t/\Lambda^2)^2$ in the matrix element (Λ^2 large). But then the behavior of the deuteron form factor would not agree with that given by quark counting at large q^2.[18] One possible solution of this problem could be that the number of resonances produced when one of the nucleons absorbs the virtual photon increases with q^2, in such a way that cancels this extra factor, and restores the q^2 dependence predicted by quark models. In fact, there are models that have this resonance behavior built in.[22]

We have also calculated form factors for other light nuclei, like He^3 and He^4. For He^3, $g = 11$, and by choosing $\delta^2_{He^3} \simeq 6$, we can fit the low q^2 data. The result is given in Fig. 10.

For He^4, $g = 17$, and with $\delta^2_{He^4} \simeq .8$, we get the curve presented in Fig. 11. It is important to have in mind that these results depend on the δ^2 value chosen in each case, which should be adjusted in order to compare with precise experimental data at larger q^2.

2. Deep Inelastic Scattering from Light Nuclei

Now that we have a relativistic wavefunction for the deuteron that has correct properties and has given good results for the form factor calculation and in inclusive reactions, including quasielastic scattering, we can apply it to other situations with some confidence. In this section we are going to describe the formalism for deep inelastic scattering from the deuteron, which

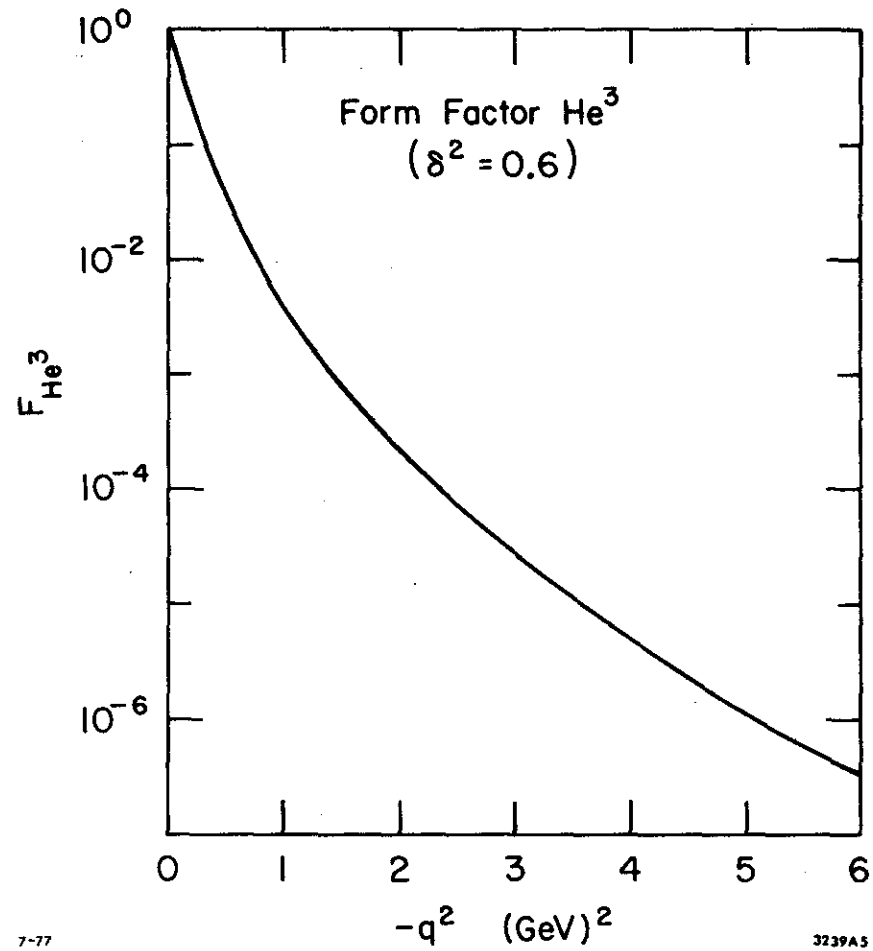

Fig. 10. Prediction for the form factor of He^3, for a specific value of the parameter δ^2 (see text).

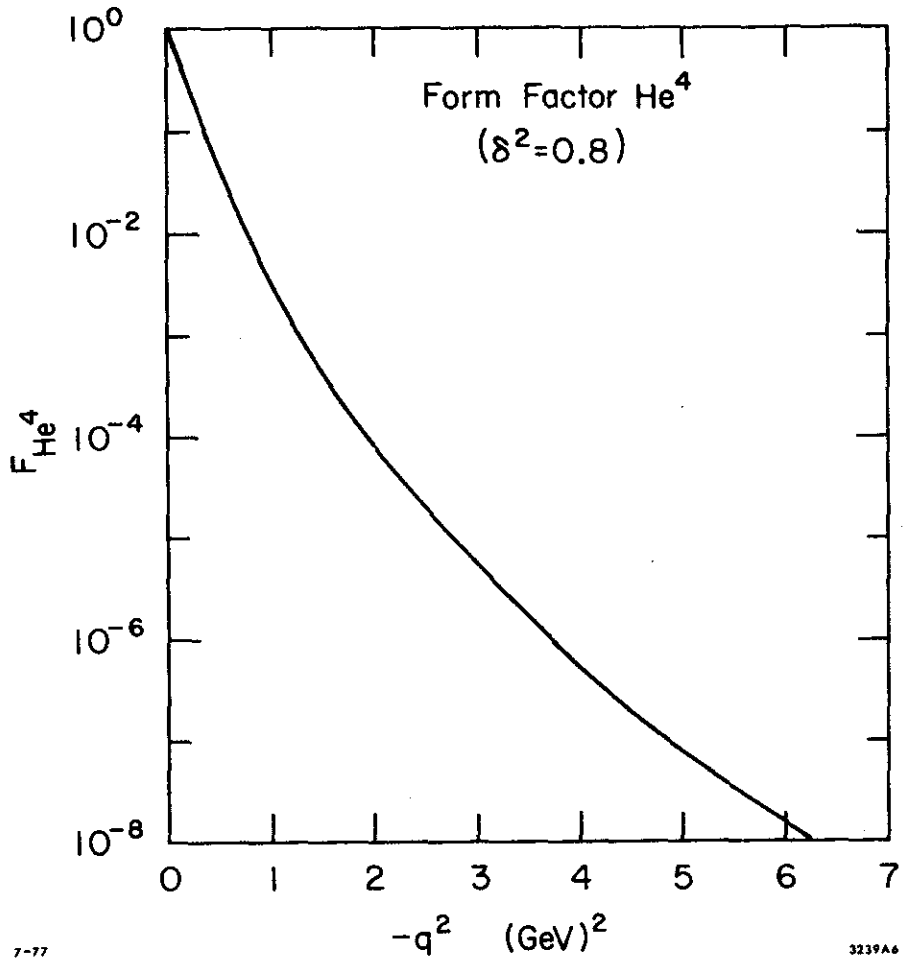

Fig. 11. Prediction for the form factor of He^4, for a specific value of the parameter δ^2 (see text).

then in the next chapter is going to be used to extract the neutron structure function from deuteron data. Although we will consider deuteron as the nuclear target, the analysis is exactly the same for other light nuclei.

We shall work in terms of the natural Bjorken variable for the deuteron

$$x_D = \frac{-q^2}{2M_D\nu} \quad ,$$

which is one-half the x defined in terms of the nucleon mass. The following procedure should be compared with that used by Atwood and West.[23]

At very large q^2, one expects that the dominant term has one quark of one of the nucleons in the deuteron absorbing the photon momentum; as q^2 decreases, more and more components of the deuteron will participate. This suggests the following classification scheme for the different contributions to deep inelastic scattering from the deuteron: (a) a highly inelastic term in which a fragment of one of the baryons recoil with momentum ~ q, the photon momentum, (b) one baryon recoils with ~ q (quasielastic scattering), and finally, (c) both nucleons recoil together (elastic or resonance scattering). This classification is described graphically in Fig. 12. Note also that the relative importance of these terms will depend, as we will see shortly, not only on q but also on the region of x_D we happen to be considering.

<u>Large q^2</u>: In this limit, the scattering from the constituent nucleons is highly inelastic and the photon momentum is absorbed by one or perhaps two quarks as we will see in the proton case. The term in which three quarks share the photon momentum will be considered separately (quasielastic scattering). Thus for large q^2 we can write (neglecting small k_T^2 effects)

$$F_{2D}(x_D,q^2) = \sum_a \int_{x_D}^{1} dy\ F_{2a}(x_D/y,q^2)\ G_{a/D}(y) \quad , \qquad \text{(IV-5)}$$

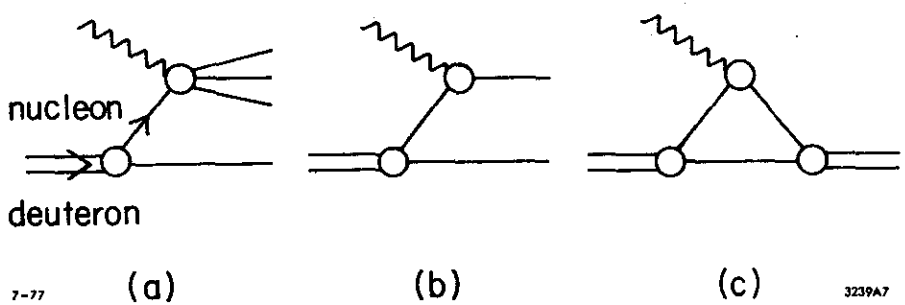

Fig. 12. Contributions to the deuteron structure function, with partons of one of the nucleons (a), one nucleon (b), and both nucleons (c) recoiling coherently.

where the sum runs over the proton and the neutron, and certain off-shell effects in F_{2a} have been neglected. This formula has been discussed in the scaling limit by Landshoff and Polkinghorne[24] for several types of reactions. Note that since $G_{a/A}(y)$ is strongly peaked at $y \sim 1/2$, for $x_D < 1/2$ one has the very approximate relation

$$F_{2D}(x_D,q^2) \sim \sum_a F_{2a}(2x_D,q^2)\ \theta(\tfrac{1}{2} - x_D) \quad , \tag{IV-6}$$

which strictly holds only in the limit of zero binding but has a simple physical interpretation. It turns out that this approximation overestimates the deuteron function by about 5%.

<u>Moderate q^2</u>: If we lower q^2, the next term that becomes important is quasielastic scattering, which should appear for $x_D \sim 1/2$. This contribution can be evaluated by the expression

$$F^Q_{2D}(x_D,q^2) = \sum_a x_D\ G_{a/D}\ (x_D)\ F^2_a(q^2) \quad . \tag{IV-7}$$

And finally the last term, which should be important for x_D close to one, corresponds to the possibility of having a final state resonance.

Explicit numerical calculations of all these terms will be presented in the next chapter, when we describe the extraction of the neutron structure function from deuteron data.

CHAPTER V. THE PROTON AND NEUTRON STRUCTURE FUNCTIONS

1. Introduction

Our nuclear scattering analysis has shown that there are coherence effects that dominate in certain regions of phase space, and which correspond to virtual emission of nuclear bound states by the interacting nuclei. It is interesting to note that in the CIM model of hadron collisions the picture is very similar, and the interacting particles emit coherent sub-systems (diquarks, mesons, baryons,...) which are the ones that give rise to the internal basic interaction. This means that there are several different terms whose relative importance will depend on the region of phase space that we are considering. In this chapter we will analyze deep inelastic scattering from protons and neutrons, using the same general ideas.

For deep inelastic events, that is, large energy (ν) and momentum (q^2) transfer, Bjorken predicted that the structure functions would remain finite and would depend only on a single variable $x = -q^2/2M\nu$. The approximate validity of this prediction[25] has had a considerable influence on the theory of hadrons, which most people consider today as being composite states of (almost) point-like objects.

The success of such a picture and the models it leads to in interpreting the major features of both weak interactions[26] and certain limiting behaviors of electromagnetic and strong interactions (the mass spectra and the large mass and large transverse momentum behavior, for example) is striking and perhaps even better than one should expect. The next problem is to find the set of fundamental theories that leads to models in the above successful class.

The observation that asymptotically free gauge theories[27] of strong interactions are capable of exhibiting scaling to within logarithmic factors whose powers are controlled by the anomalous dimensions in the theory[28] was an important step in this direction. The next question is whether or not these theories can quantitatively fit the various features of the data. This task has been undertaken by several groups who have stressed the importance of studying the nonscaling, or rather the approach to (approximate) scaling, behavior of the inelastic structure functions and of comparing features of the observed behavior with the predictions of a basic theory. In particular, Tung[29] has compared the predictions of asymptotically free theories to those of conventional theories and De Rujula, Georgi and Politzer[30] have examined and defended a study using asymptotically free QCD theory in a series of papers and talks. The practical problems of carrying out such a program have been discussed by Gross, Treiman and Wilczek[31] who have examined uncertainties in making mass dependent corrections. Other authors[32] have discussed possible difficulties in using perturbation theory with the operator product expansion. This program is indeed an extremely important one for weak, electromagnetic, and strong interactions.

Our purpose in this chapter is quite modest in comparison to the total program of the above authors. We only wish to point out that there are certain scale breaking effects that are very simple from a physical point of view and which would seem to be present in any theory susceptible to a parton interpretation. These terms are *a priori* expected to be important for large x, the Bjorken scaling variable. At small x, they do not necessarily dominate from general arguments and there are many additional effects that could become important. Indeed, the data indicates that the terms under consideration are certainly not dominant there.

These contributions show up first in the twist-6 terms in the language of the operator product expansion and would thereby be normally neglected. However they would be expected to be large from physical arguments. While they fall rapidly in q^2, their coefficient is expected to be large. They do not correspond to interference terms between various final state configurations that prefer to populate different regions of the final phase space. If such "trivial" scale breaking terms are present in the data with its necessarily finite q^2 range, it is certainly important to recognize their effect before asking more fundamental and specific questions of such data since these terms should be present in almost any theory.

In order to separate the terms that contribute, we will follow the same classification scheme as in the deuteron case, which is based on the idea that as q^2 increases more and more substructure is revealed in the hadronic bound state. The different contributions to the structure function are most easily described in the parton-quark language. The structure functions will be written as a sum over final states in which all the quarks have low transverse momenta except for (a) one quark which recoils with momentum $\approx q$, (b) two quarks that recoil with a total of $\sim q$ but each has a finite fraction of q, (c) three quarks that recoil with a total of $\sim q$, etc. The above classification neglects the coherence between such states and should be applicable for sufficiently large q values where the final configurations become incoherent. The importance of type (b) terms, for example, will be shown to be the fact that while they fall in q^2 at fixed x, they vanish less rapidly than type (a) terms for fixed q^2 as $x \to 1$. We should point out that the partons in our model do not have form factors as

used in the extended parton model of Chanowitz and Drell[33] (but our two quark system does).

One point worth mentioning is that there are many variables that asymptotically become equal to the Bjorken x, and which make data at small q^2 satisfy scaling to different degrees. An often used one is the Bloom-Gilman x' ($= x(1+M^2/2M\nu)^{-1}$). Most of these improved scaling variables, however, do not have a clear theoretical significance. We shall neglect such effects for the most part, although an estimate of both mass and initial state effects will be mentioned. Our purpose is to see if one can fit the approach to scaling with terms that have a clearer and more direct physical interpretation.

2. Proton Structure Function

In order to illustrate the physical point that we wish to make without obscuring the issue with algebra, we will treat only the spin averaged case and hence will neglect the spin of the quarks in the formulation of the model. Following the classification discussed in the introduction, the contributions to the proton structure function to be considered here are illustrated in Fig. 13. Our analysis is very much in the spirit of the CIM model of hadron collisions,[11] in the sense that it is clearly necessary to consider all possible final states in order to extract those configurations that are expected to dominate in a particular region of phase space. And also as in the CIM, we shall use dimensional counting to predict the behavior of form factors and generalized structure functions.[14]

In Fig. 13a, one quark absorbs all the momentum q carried by the virtual photon. This is the dominant diagram of the parton model. In Fig. 13b, the photon is absorbed by a two quark system which then recoils, each quark having

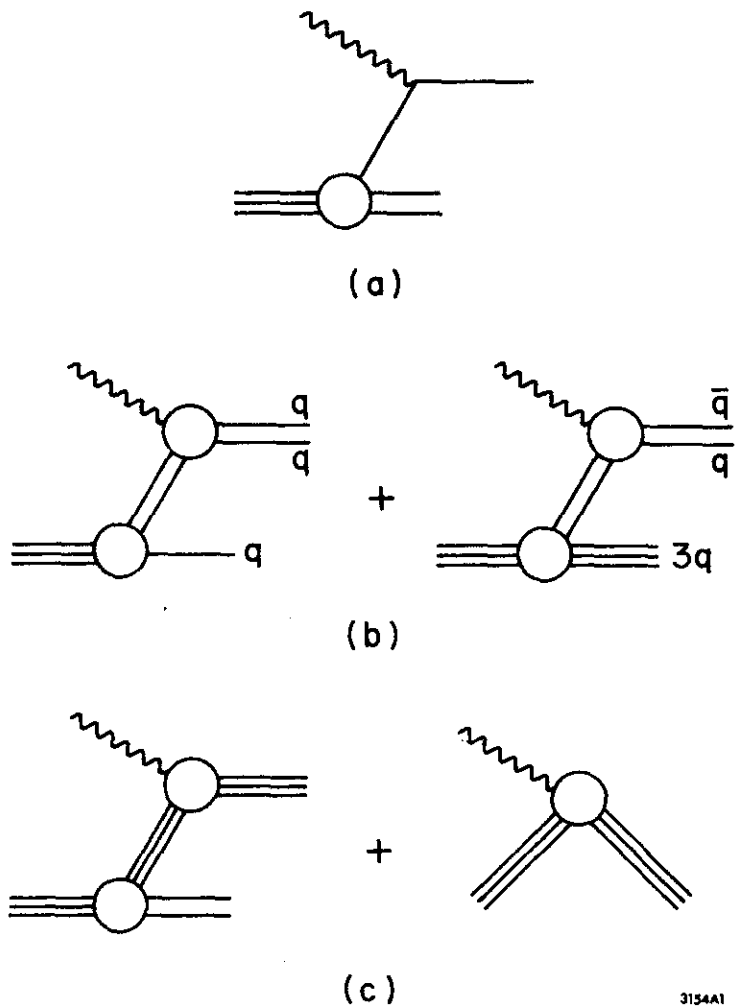

Fig. 13. Contributions to the proton structure function, with one (a), two (b), and three (c) quarks recoiling coherently.

a finite fraction of q. This diquark state need not be thought of necessarily as a bound system, but a photon striking a virtual meson in the target that remains bound will also be of this type. In Fig. 13c, the photon is absorbed by a triquark, or baryon, system and this obviously involves the form factors for nucleon elastic scattering and resonance production. This latter contribution is very small in the region of interest and will be neglected.

Since the diagram in Fig. 13a approximately scales, for the present purposes its contribution to $\nu W_2(x)$, or rather $F_2(x)$, will be written in the form

$$F^V_{2p} = A_V(x)\ (1-x)^3 \quad , \qquad \text{(V-1)}$$

where the $(1-x)^3$ dependence is given by dimensional counting (two spectator quarks). Here $A_V(x)$ is a rather slowly varying function of x (for large x) which is expected to behave such that the most likely valence quark momentum is near (or less than) 1/3. Since it describes the interaction of valence quarks, it must vanish for $x \to 0$ (Regge behavior). $A_V(x)$ may also be a very slowly varying function of q^2. Such slow variations can arise from a fundamental scale breaking, such as QCD, or from the kinematic effects of the binding of the quarks. This latter effect could be called a mass effect, an off-mass-shell effect, or a wavefunction effect, as the reader prefers. It has been estimated using a choice for the relativistic bound state wavefunction that was successful in the nuclear case of the previous chapters. We find an effect which for large x goes in the opposite direction from that to be discussed shortly. Such effects will be neglected here but if they were included, they would simply increase the normalization of our explicit nonscaling term. Our object here is to see if the observed scale breaking at moderate and large x values ($x \gtrsim 1/3$) can be explained with an $A_V(x)$ that does not depend strongly on q^2. At small x ($\lesssim 1/3$), however, such wavefunction

effects could be more important, providing all or part of the increase with q^2 of F_{2p} that is seen experimentally.

There is also another contribution in which only quark (or antiquark) interacts, but in this case that quark belongs to quark-antiquark pairs in the parton sea. This means that this term must be constant for $x \to 0$ (pomeron behavior), and since the number of spectator quarks now is four, it must vanish as $(1-x)^7$ for $x \to 1$. Then we write it in the form

$$F_{2p}^{sea}(x,q^2) = A_s\ (x,q^2)\ (1-x)^7 \quad . \tag{V-2}$$

Since this term is only important at small x, where there are many effects that could be present (Regge, asymptotic freedom, wavefunction effects, etc.), the q^2 and x dependence of $A_{sea}(x,q^2)$ will be found by directly fitting the experimental data.

In the first diagram of Fig. 13b, the photon is absorbed by a diquark system that has a form factor $F_d(q^2)$ that falls as $1/q^2$ from dimensional counting. The x-dependence is quite easy to infer from the graph. This contribution must vanish as $(1-x)$ for $x \to 1$ since there is only one spectator quark. Now the most likely diquark momentum fraction is ~2/3, and this follows automatically if the nonscaling term is chosen to have the form calculated for valence constituent:

$$F_{2p}^{d}(x,q^2) = A_d F_d^2(q^2)\ x^2(1-x) \quad . \tag{V-3}$$

This has all the desired limiting properties if F_d is parametrized as

$$F_d(q^2) = d^2(d^2-q^2)^{-1} \quad . \tag{V-4}$$

Note that if a virtual meson absorbs the photon and remains bound, as in the second diagram in Fig. 13b, the structure function will have the same q^2 dependence as above arising from the pion form factor but it will fall as

$(1-x)^5$. It is estimated to have a small overall normalization for $x > 1/3$. Hence it will be neglected in our fits.

The total structure function in this approximation is

$$F_{2p} = F_{2p}^{v}(x) + F_{2p}^{d}(x,q^2) + F_{2p}^{sea}(x,q^2) \tag{V-5}$$

and higher terms have been neglected. Fits to the proton data[34] are shown in Fig. 14, and one sees that it is possible to have both a consistent and simple picture of the approach to scaling in this framework for large enough x and $(-q^2) \gtrsim 2(\mathrm{GeV})^2$. If scale breaking is to differentiate between specific basic theories, it evidently must be studied at small x, say $x \lesssim 0.3$, not at large x where the observed scale breaking can be simply explained in terms of physically expected effects in any scale invariant theory with even an approximate parton interpretation. This is not to say that our term necessarily explains all the scale breaking observed in this region, but without prior prejudice and information, it is not possible to decide how much is to be ascribed to the more fundamental (and interesting) properties of the theory under consideration.

The parameters used in the above fits are $A_d = 2.5$, $d^2 = 2$. $A_V(x)$ is quite slowly varying for large x, with an average of ~ 0.8. Graphs of $F_{2p}(x,q^2 = -\infty)$ and $A_V(x)$ are given in Fig. 15. A possible fit to $A_V(x)$ is

$$A_V(x) = \begin{cases} 1.58\ x^{0.6} & (0 \le x \le 1/3) \\ 1.58\ x^{0.6}(0.93-0.85|x-2/3|-1.15(x-2/3)) & (1/3 \le x \le 1)\ . \end{cases} \tag{V-6}$$

The value of d^2 we find uncomfortably large, but it is necessary in order to fit the data at small q^2 ($\gtrsim 2$). A value of $d^2 = 1$ fits for $q^2 \gtrsim 3$. Since $A_V(1) \neq 0$, F_2 satisfies the Drell-Yan-West relation for $x \sim 1$.

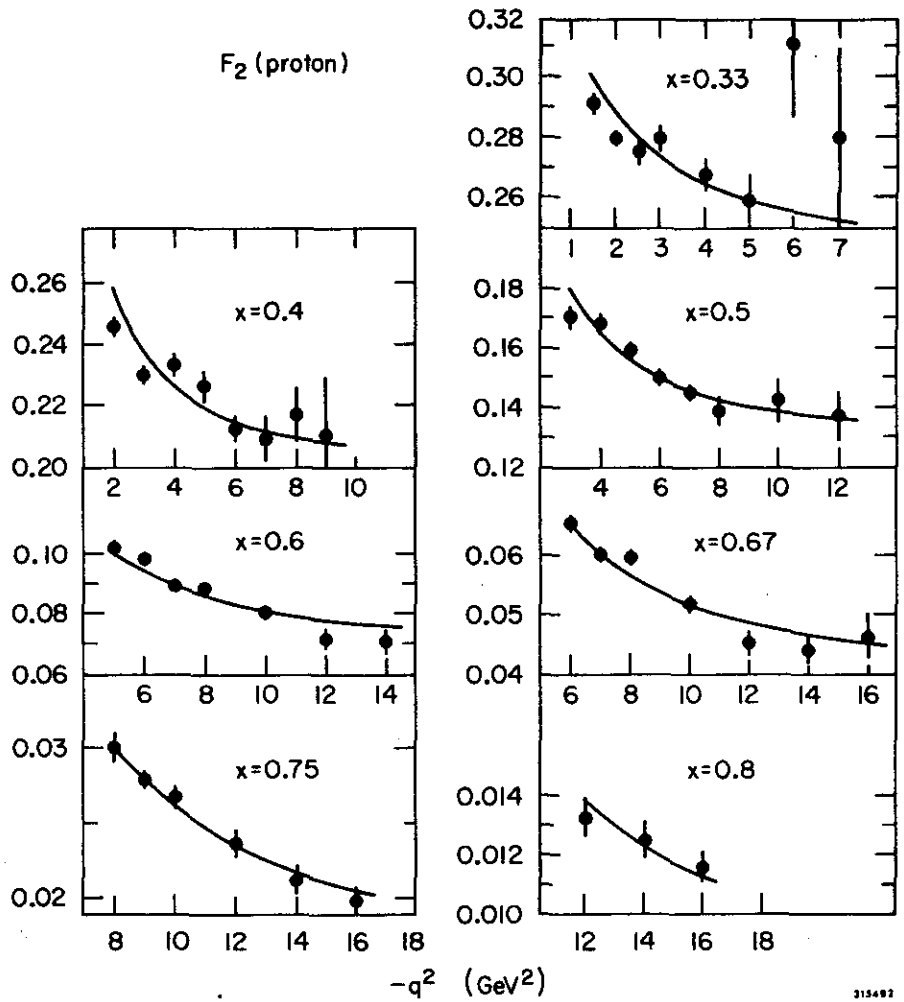

Fig. 14. Fits to the data of the proton structure function $F_{2p}(x,q^2)$, for different values of x, as a function of q^2. See Eq. (V.5).

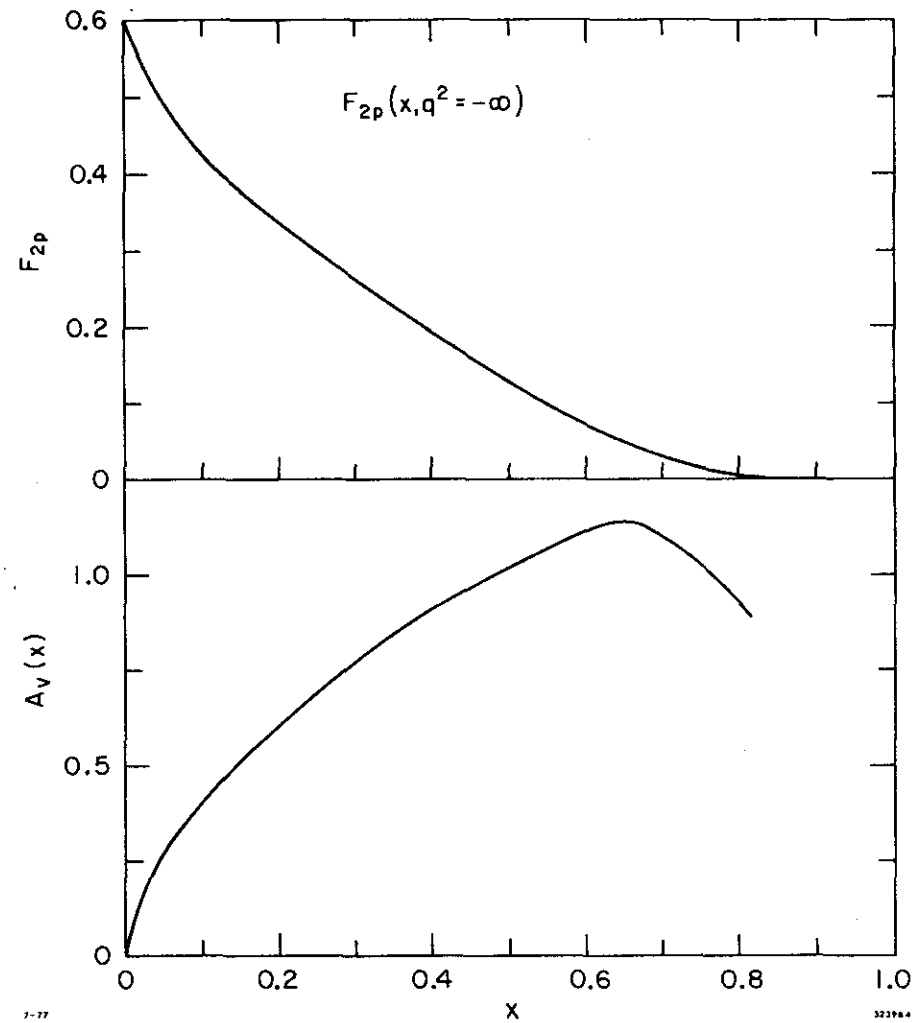

Fig. 15. Scaling part of the proton structure function ($F_{2p}(x,q^2 = -\infty)$), and coefficient $A_v(x)$ of the valence contribution.

Our fitting of the small x region yields the form[35]

$$A_s(x,q^2) = (0.6 - \sqrt{x})(1 - 2F_d^2(q^2)) \qquad \text{(V-7)}$$

for $x < .36$, and zero otherwise. Since we have considered only the region $(-q^2) \gtrsim 2(\text{GeV})^2$, the fact that this term becomes negative for small q^2 has no significance and should not be taken seriously. We chose the same function F_d as in the diquark term to parametrize the q^2 behavior of this sea contribution because experimentally the first moment of the structure function is independent of q^2 in the range $2 < (-q^2) < 30(\text{GeV})^2$.[34] Notice that this particular form makes F_{2p} increase with q^2 for small values of x, while the diquark term makes it increase for large x, as seen experimentally. In fact, we have calculated the first moment using our parametrization, and obtained $\int_0^1 F_{2p}\, dx \approx .17$, constant for $q^2 \gtrsim 5(\text{GeV})^2$. As expected, this result agrees very well with the data.[34] At this point we should mention that the asymptotic freedom prediction with respect to this first moment is a logarithmic fall-off, which will have to be quite slow in order to reproduce the experimental data.

While the data[34,36] for F_1 has not been fully analyzed, we have found that the valence terms in F_1 and F_2 extracted by the above procedure agree better with the Callan-Gross[37] relation ($x F_1^V = F_2^V$) than the total structure function at low q^2. Since the diquark term is an effectively integer spin object, it could break this relation for the full (unseparated) structure functions in regions where it is important.

3. <u>Drell-Yan-West Relation</u>

The threshold limit of the structure functions should be smoothly connected, in the sense of Bloom-Gilman duality,[38] to the elastic or resonance form factors $G(q^2)$. According to the Drell-Yan-West relation,[13] as x approaches one from below ($x = 1 + (m^2 - M^2)/q^2$, where m is the missing mass and M is the proton mass), one has

$$(-q^2)\, G_{Mp}^2(q^2) \approx \int dm^2\, F_{2p}(x,q^2)$$

$$q^8\, G_{Mp}^2(q^2) \sim \int dm^2 \left[A_v(1)(m^2 - M^2)^3 + A_d d^4 (m^2 - M^2)\right] , \qquad \text{(V-8)}$$

and the integral runs roughly from the nucleon mass M up to the effective threshold for pions.[39] Thus the nonscaling terms contribute to the leading asymptotic behavior of the form factors and for our fit, dominate. The above is clearly not the complete story since there are other contributions, especially interference terms, that become coherent in the limit $x \to 1$ and also contribute to leading order in q^2. This is necessary since G must contain a coherent sum over charges, whereas the contribution to the usual structure functions involves the sum of the squares of the charges of the elementary constituents. The nonscaling terms A_d contain some of the interference effects, but not all. In any case, the relation (V-8) is approximately satisfied if m is integrated from M to the threshold for two pions, $M + 2\mu$.

Finally, we note that if the above connection also holds for the neutron, with the same integration region and $G_p(q^2)/G_n(q^2) = \text{constant}$, then if the scaling term dominates one has $(\mu_n/\mu_p)^2 \approx \left(A_v^n(1)/A_v^p(1)\right)$, whereas if the nonscaling term dominates, which is the case in our fits, then $(\mu_n/\mu_p)^2 = \left(A_d^n/A_d^p\right)$. Otherwise the value is an intermediate one. Our fit for the first ratio will be shown in a later section to be ~0.40, whereas the ratio for

ıe nonscaling term is ~0.33. Both of these are somewhat below the square of ıe experimental ratio of magnetic moments (~0.47) but are consistent within ıe errors of our extraction. This relation is not to be taken too quantiatively due to the coherence problems alluded to above.

. The Neutron Structure Function Extraction

In order to analyze the neutron structure function and see if its properies agree with our general model of scale breaking, we will first extract it rom deuteron data. This extraction will be done using a fully relativistic odel for the deuteron, which we do not believe has been done before. The ormalism for deep inelastic scattering from the deuteron was developed in he previous chapter, so here we will apply it and present the numerical esults.

Large q^2: Following the classification given in Section (IV-2), in this limit the photon momentum is absorbed by one or two quarks in one of the ıucleons of the deuteron.

Since the distribution function $G_{a/D}(x)$ is known with some accuracy, Eq. (IV-5) will be used to extract the neutron structure function $F_{2n}(x,q^2)$ from the large q^2 deuteron data. In order to carry out the fit in a convenient form, define

$$F_{2n}(x,q^2) = F^v_{2n}(x) + F^d_{2n}(x,q^2) + F^{sea}_{2n}(x,q^2) \quad , \qquad \text{(V-9)}$$

where

$$F^v_{2n}(x) = B_1(x)\ F^v_{2p}(x)$$

$$F^d_{2n}(x,q^2) = B_2(x)\ F^d_{2p}(x,q^2) \quad ,$$

$$F^{sea}_{2n}(x,q^2) = F^{sea}_{2p}(x,q^2) \quad ,$$

and where, due to the isoscalar character of the parton sea, the last term is the same for protons and neutrons. A fit to the data can be achieved with the $B_1(x)$ given in Fig. 16 and with $B_2(x)$ = constant = 1.3. Error bars in the graph for $B_1(x)$ are due to uncertainties in the experimental data. Also in Fig. 16 we show the asymptotic ratio R of neutron and proton structure functions. We have restricted the extraction to $x_D < 1/2$ in order to decrease the sensitivity to the assumed form of $G_{a/D}(y)$. The resultant fit to data[34] in this region is given in Fig. 17. The separate parts (valence, diquark, sea) of the neutron and proton structure functions and their sum are given in Fig. 18 for $q^2 = -5(\text{GeV})^2$, and in Fig. 19 we compare the asymptotic values for the resultant total proton and neutron structure functions with the results obtained for $q^2 = -5(\text{GeV})^2$.

There are several points worth mentioning. The function $B_1(x)$ is slowly varying over the range of x considered, $x \gtrsim 0.1$. The average value of $B_1(x)$ around the valence peak (x = 1/3) is roughly consistent with 2/3 which is the ratio of the sum of the squares of the valence quark charges, neutron/proton = (2/3)/1. The ratio of the asymptotic neutron to proton structure functions decreases for large x, and the extrapolation seems to give the value of $\approx 1/4$ at x = 1, which is the lower bound that holds in the valence quark model.[40] At x = 0, on the other hand, this ratio goes to 1, which reflects the isoscalar character of the parton sea. The value of 1/3 found for $B_2(x)$ is the ratio of the sum of the squares of the valence diquark charges, neutron/proton = (2/3)/2. (A slightly better fit can be obtained by taking $B_2(x)$ to be slowly varying, with an average value of 1/3.) These features of the fit are evidence of the consistency of our interpretation and fit (but certainly not its uniqueness).

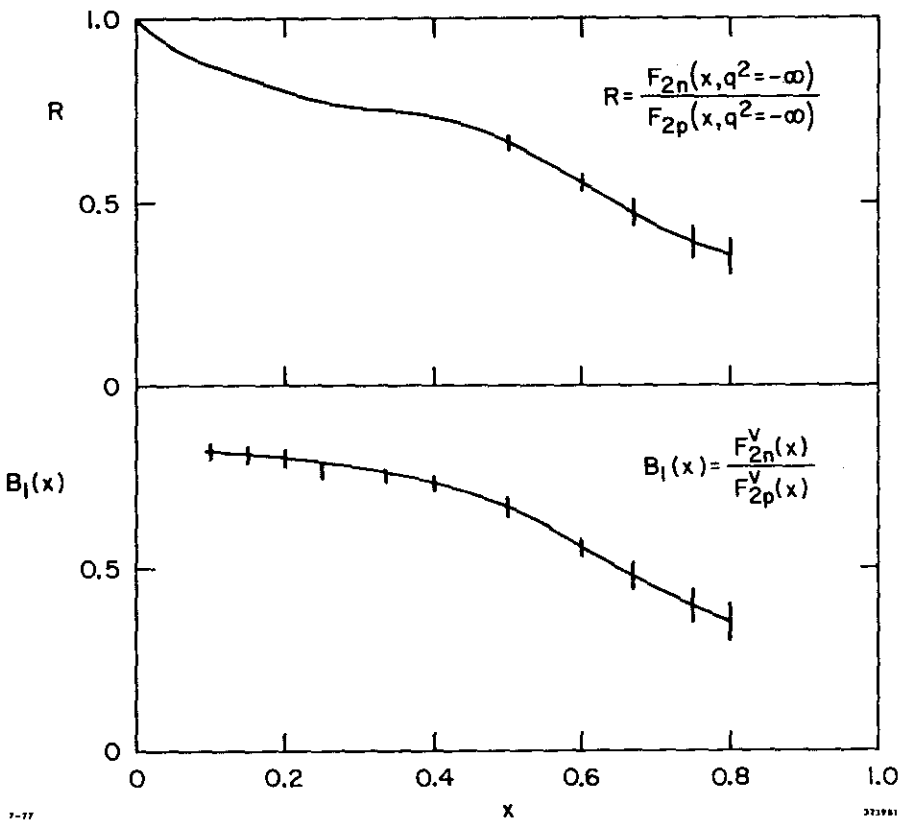

Fig. 16. Ratio of the asymptotic structure functions of proton and neutron $F_{2n}(x,q^2=-\infty)/F_{2p}(x,q^2=-\infty)$, and ratio of the valence parts $F^V_{2n}(x)/F^V_{2p}(x)$.

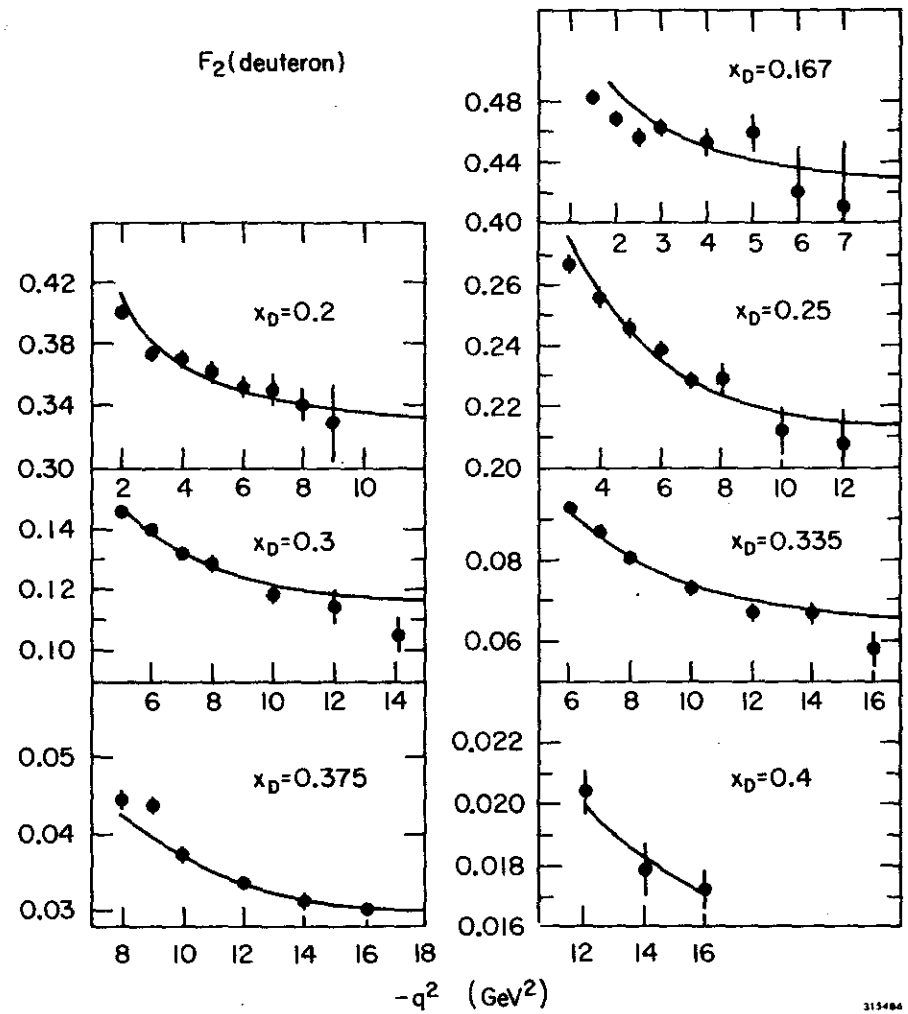

Fig. 17. Fits to the deuteron structure function $F_{2D}(x,q^2)$, for different values of x, as a function of q^2, which were used in the extraction of the neutron data.

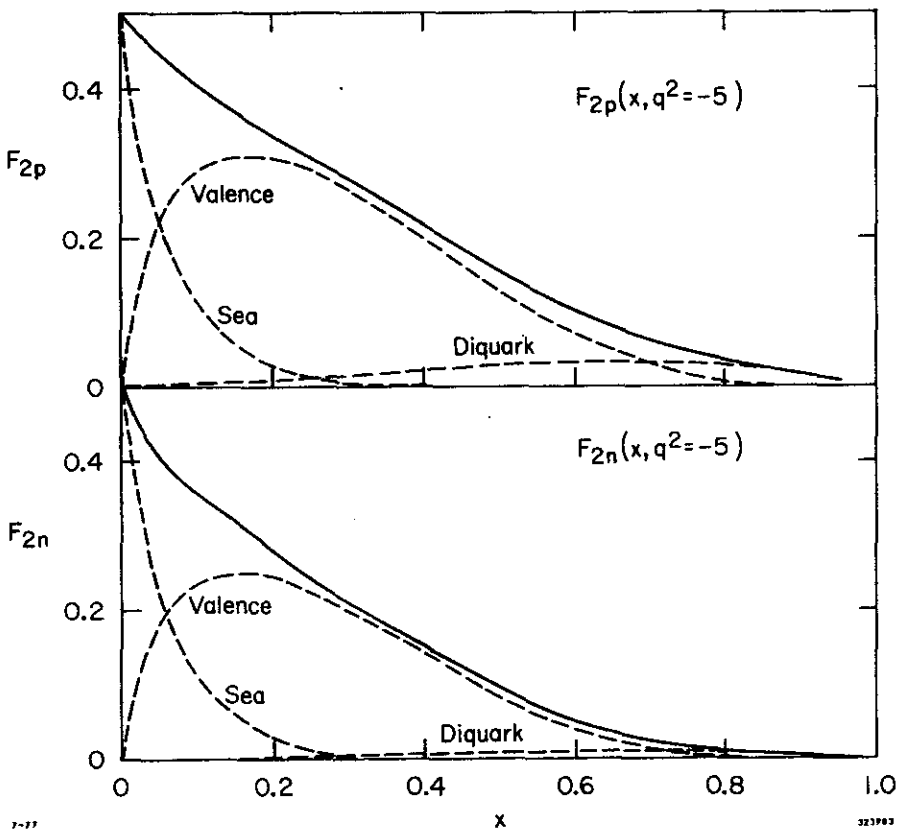

Fig. 18. The contributions (valence, diquark and sea) and the total structure functions of proton and neutron (for $q^2 = -5\ (\mathrm{GeV})^2$).

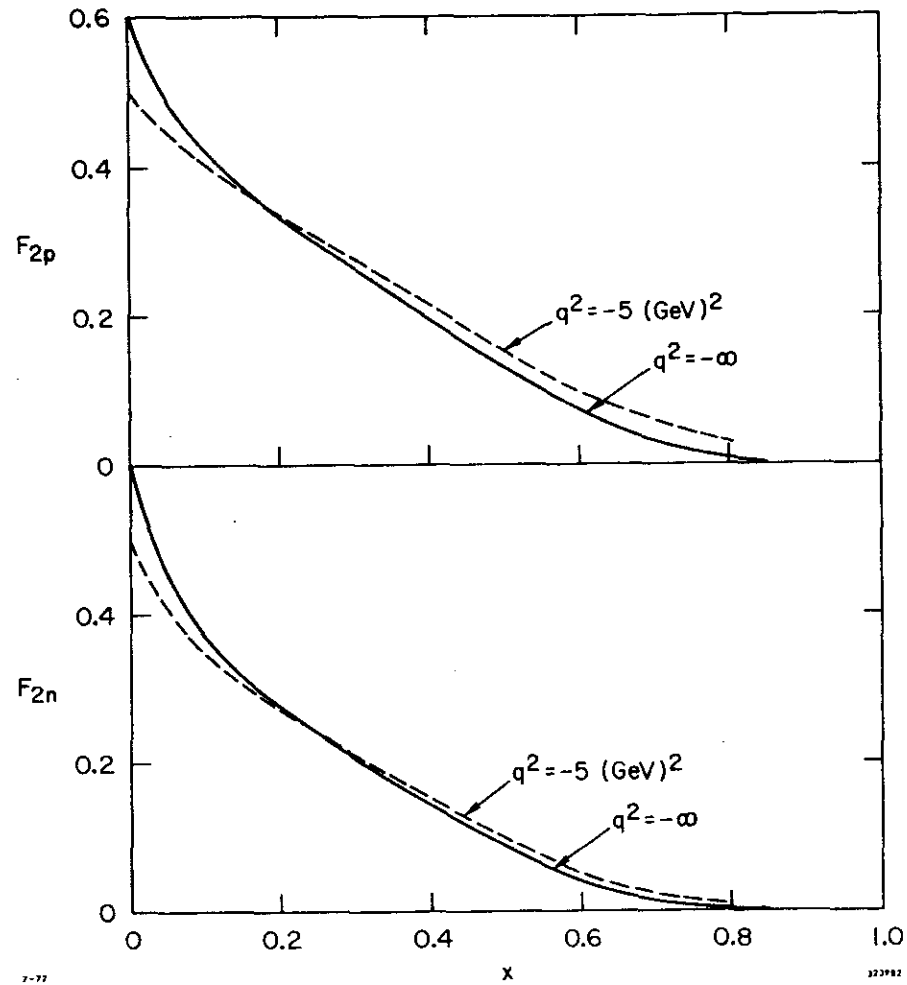

Fig. 19. The proton and neutron structure functions, for $q^2 = -5\ (\mathrm{GeV})^2$ and $q^2 = -\infty$.

In performing our extraction of the neutron structure function we have used a distribution function $G_{a/D}(x)$ which is symmetric around $x = 1/2$. This fixes $N(x)$ in Eq. (IV-2) to be $N(x) = N_0 x^2$. We have also tried $N(x) =$ constant, which does not change noticeably the fit to the deuteron form factor, but which gives a somewhat larger $B_1(x)$ in the large x region. Although the symmetric model is more realistic, this result means that there is some extra uncertainty in the extraction. Measurements of the quasielastic peak in deuteron deep inelastic electroproduction, and of the deuteron form factor at larger values of q^2 would be very useful in determining the correct form of $N(x)$.

Moderate q^2: Using only the above terms, we can now compute $F_{2D}(x_D, q^2)$ for all values of x_D using Eq. (IV-5). The result labelled inelastic is given in Fig. 20 at large q^2 and in Figs. 21 and 22 at moderate q^2 as a function of

$$\omega' = \frac{1}{2x_D} - \frac{M^2}{q^2} \quad ,$$

which has been used in the presentation of the data of Schütz et al.[41] At this stage our curve for the inelastic contribution falls below the present data for $(-q^2) \gtrsim 2(\mathrm{GeV}/c)^2$ for $1 > \omega' > 1/2$ $(x_D \to 1)$. This is not surprising since the quasielastic and fully coherent "resonance" contributions have not been included. Quasielastic scattering should be important for $x_D \sim 1/2$ and for the lower range of q^2 values.

This contribution which should be added to the $F_{2D}(x_D, q^2)$ given by Eq. (IV-5) is

$$F^Q_{2D}(x_D, q^2) = \sum_a x_D \, G_{a/D}(x_D) \, F^2_a(q^2) \quad . \qquad \text{(V-10)}$$

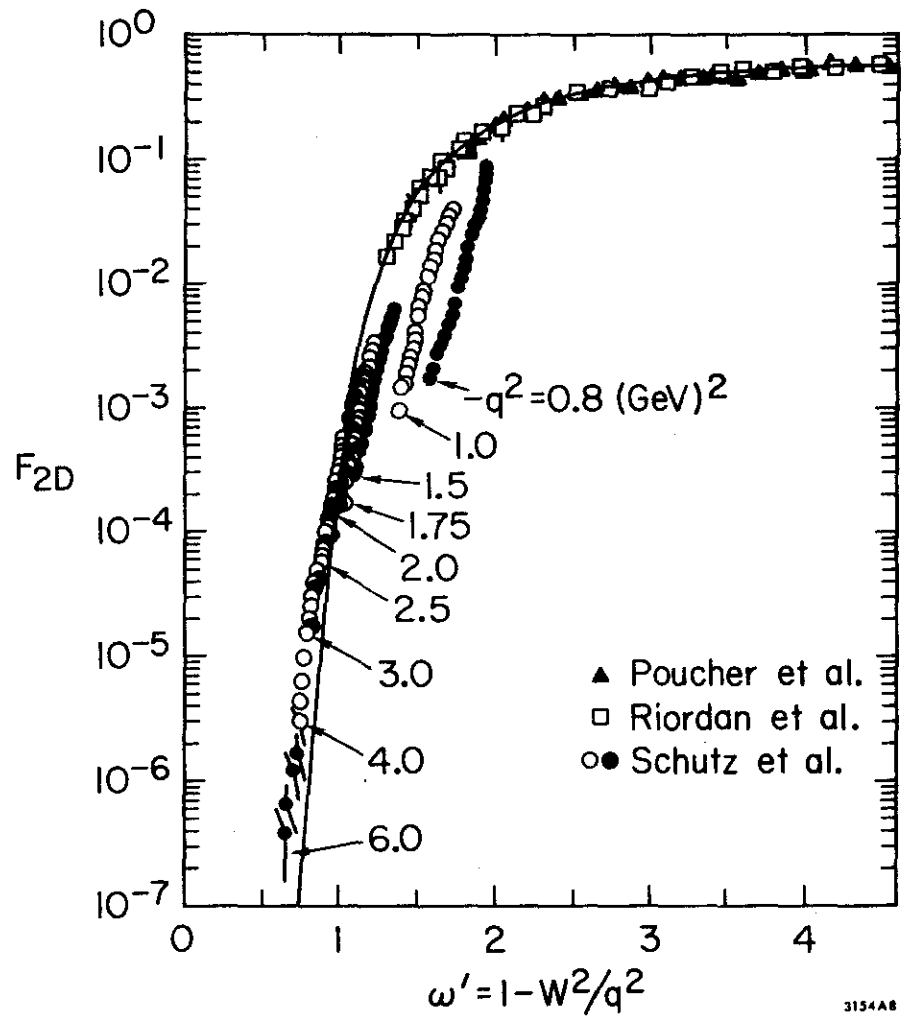

Fig. 20. Prediction for the deuteron structure function for very large q^2. The data is from Refs. 34 and 41.

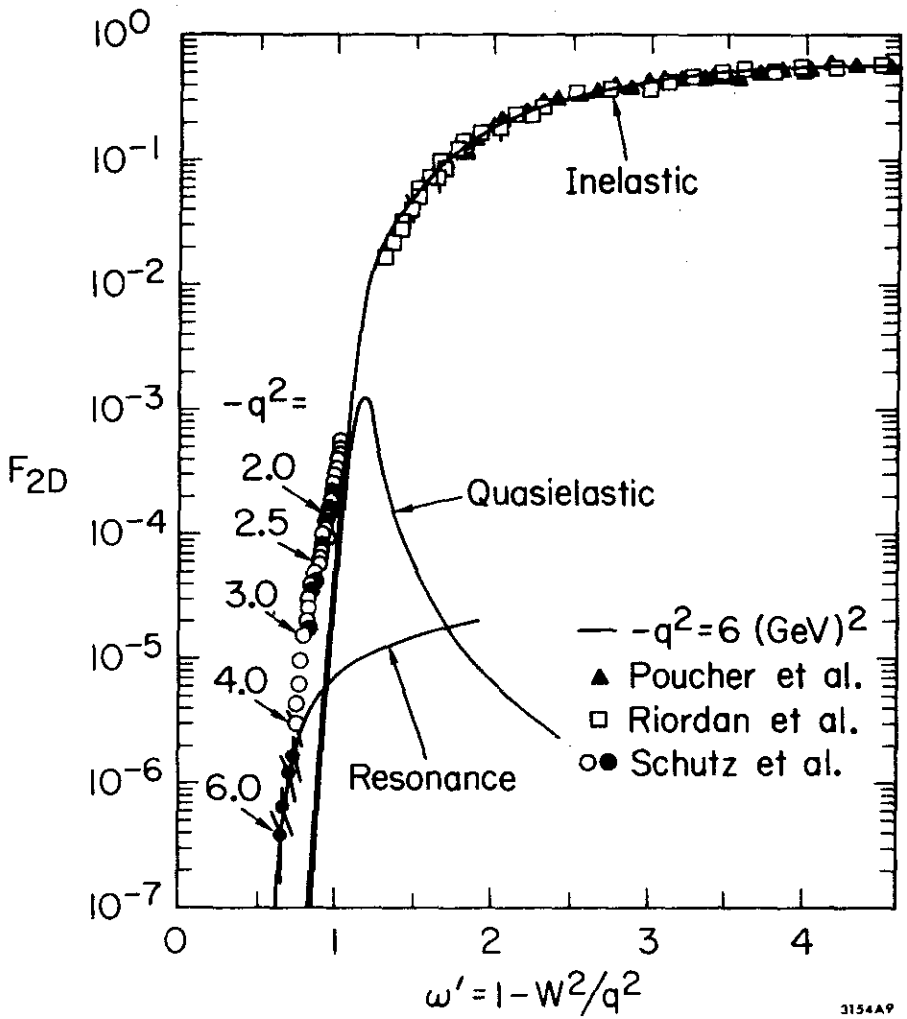

Fig. 21. The three contributions to the deuteron structure function (inelastic, quasielastic, resonance), for $q^2 = -6$ (GeV)^2.

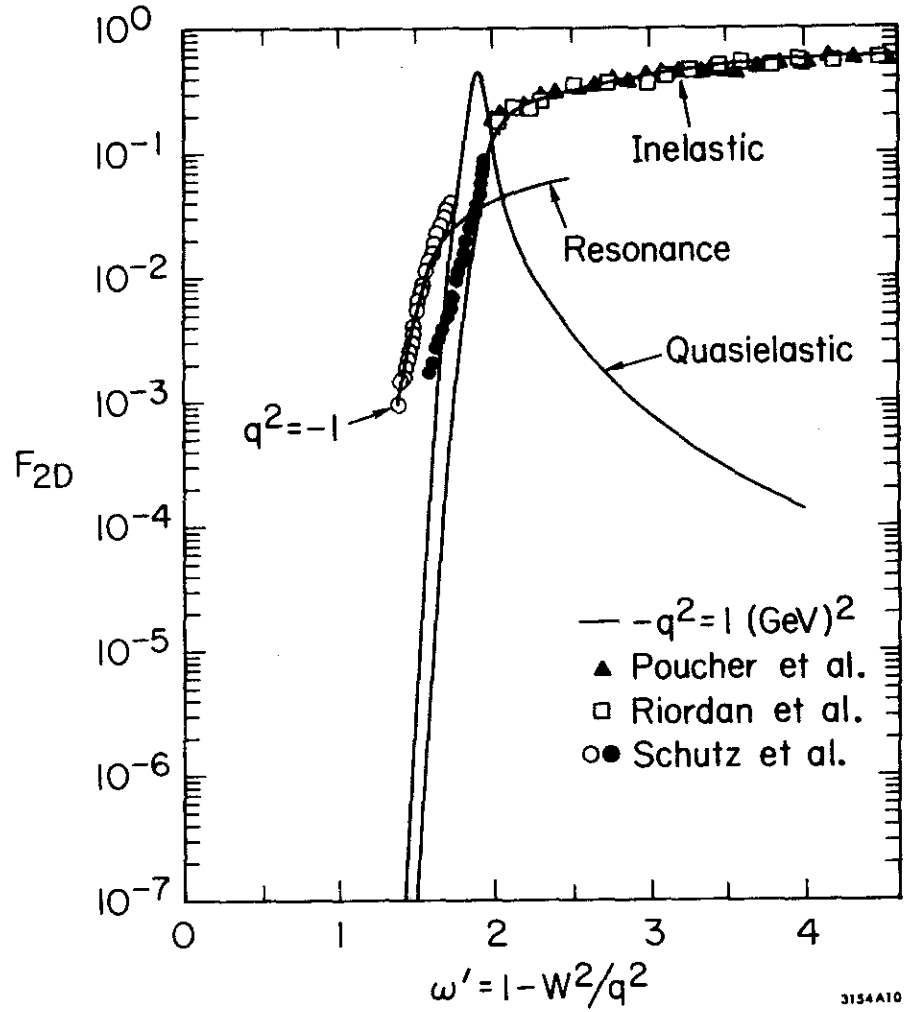

Fig. 22. The same three contributions for $q^2 = -1$ (GeV)^2.

It has been plotted separately in Figs. 21 and 22 for $(-q^2) = 6$ and $1(\mathrm{GeV}/c)^2$ respectively. For the smaller q^2 value there is a clear quasielastic peak which has been suppressed at the larger q^2 by the nucleon form factor. It would be very interesting to have data in this region to explore the properties of the quasielastic peak.

In the region of x_D very close to one, the data are clearly larger than the sum of the contributions considered so far, even if the experimental resolution is used to smear the prediction. In Ref. 41, the suggestion is made that this could be due to a final state resonance in which the two nucleons share the momentum of the virtual photon. This contribution can be fitted to the data if written in the form

$$F^R_{2D}\left(x_D, q^2\right) = (-q^2)\ F^2_D(q^2)\ 10^{3-2x_D^2} \qquad \text{(V-11)}$$

which for $q^2 = -6$ and 1 is shown in Figs. 21 and 22. We are not sure that this is a correct interpretation but a contribution which roughly has the above structure was predicted by Jankus[42] in scattering from the deuteron near the inelastic threshold. Jankus found a strong localized enhancement in this region that was due to nonresonant (scattering length) final state interactions. Such an effect was found experimentally.[43] It would be very interesting to compute this effect with a relativistic treatment of the deuteron to check its consistency with the data. A different approach to fitting this data has been described by Frankfurt and Strikman.[44]

5. Conclusions

In this chapter we have shown that the ordinary parton model, which normally is assumed to scale (except for mass corrections), has physically identifiable terms that do not scale. The final states that were of most

interest here were one quark recoiling with the photon momentum and two quarks sharing this momentum. The predicted form of the structure functions and form factors for these terms were shown to provide a reasonable fit to the proton and neutron data for $x \gtrsim 1/3$ and $(-q^2) \gtrsim 2(\mathrm{GeV})^2$. The ratios between the proton and neutron are as expected in the model. Due to the uncertainties involved, our parameters should be considered as having "typical" values. The errors are correlated between the parameters of the scaling and nonscaling terms and no systematic error analysis has been made.

Our model and fit is certainly not the only way to understand the nonscaling behavior of the structure function at large x. This behavior is also fitted by using "ξ-scaling"[45] plus asymptotic freedom models.[29,30] There should be experimentally measurable differences between this approach and ours, however. While we do not know precisely what the latter models predict, if our explanation is correct there should be protons in the photon fragmentation region for large x. The single quark recoil or scaling term should prefer to decay to mesons (the leading mesons would then have a (1-x) decay function behavior). The diquark recoil term should decay not only to mesons but also should decay strongly to baryons (the leading baryons should also have a (1-x) decay function behavior). Therefore if our explanation is correct, the proton/pion ratio should follow the ratio of the nonscaling term to the full structure function. The observation of recoil protons arising from a preferred x value of 2/3 and a q^2 behavior of $(-q^2)^{-2}$ would be confirmation of our general picture. The absence of such protons may be more consistent with asymptotic freedom models. At the present time, the proton/pion ratio cannot be predicted since we do not know the decay probability functions for a diquark system to produce pions and protons.

These functions can be measured in principle in several independent ways, however, such as in e^+e^- annihilation and in the target fragmentation region of deep inelastic lepton scattering.

The scaling terms in F_1 and F_2 were found to be in reasonable agreement with the Callan-Gross[37] relation. If the diquark system is predominantly spin one, then one expects large asymmetry effects in deep inelastic lepton scattering with polarized beam and target.[46]

It is clearly possible to ascribe the lack of scaling at large x to either our model or to asymptotic freedom models or to any combination. This is not the case at small x. Our model is not able to explain the probable rise in q^2 at small x of the structure function suggested by high energy μ-scattering[47] or the nonscaling behavior at small x seen in neutrino scattering.[48] (A general fit to all this data has been given in Ref. 49.) This behavior is strong evidence for asymptotic freedom and/or the production of new, heavy quarks, and/or Regge-duality effects,[50] but this is unfortunately in a region where it is difficult to make quantitative calculations. However, since the diquark terms can be used to decrease the size of the nonscaling effects due to asymptotic freedom at large x, then there may not be enough rise left at small x to explain the data in such theories.

A relativistic model of the deuteron has been developed and used to extract the neutron structure functions. We do not believe this has been done before. Our method is easily susceptible to a more accurate treatment (especially important here would be the inclusion of spin effects). We have checked our deuteron model by comparing it with the measured elastic form factor and inelastic data for all x_D.

To conclude, we have shown that a simple extension of the parton model, together with dimensional counting, provides a reasonable fit to the nonscaling behavior of the proton and neutron structure functions for x larger than the valence quark peak at 1/3.[51] The model can be tested by looking at the proton yield in the photon fragmentation region. We therefore conclude that if one wants to differentiate between basic theories of hadrons by studying only the structure functions, it must be done at small x where the above nonscaling terms are probably unimportant. Even in this region of x, however, one is faced with the problem of demonstrating that such effects are indeed small, especially if one is making a quantitative comparison with a particular basic theory.

REFERENCES

1. For a review see B. Cork, in Proc. of the Int. Conf. on High Energy Physics and Nuclear Structure, Los Alamos, 1975, p. 598. Also H. Steiner, in High Energy Collisions Involving Nuclei, G. Bellini, L. Bertocchi, and P. G. Rancoita, eds. (Editrice Compositori, Bologna, 1975), p. 151.
2. J. Papp et al., Phys. Rev. Letters 34, 601 (1975).
3. J. Papp, Ph.D. Thesis, University of California, Berkeley, Report LBL-3633 (1975).
4. L. S. Schroeder, Report LBL-3362, presented at the Particles and Fields Meeting of the American Physical Society, Williamsburg (1974).
5. A. M. Baldin et al., Sov. J. Nucl. Phys. 18, 41 (1974).
6. G. F. Chew, Print-75-0222, University of California, Berkeley. This analysis is in terms of triple Regge theory. One can interpret our results as predictions of the values of "effective" Regge trajectories. See alo F. Uchiyama, in Proc. High Energy Heavy Ion Summer Study, Lawrence Berkeley Laboratory, 1974, p. 293.
7. H. Feshbach and K. Huang, Phys. Lett. B 47, 300 (1973).
8. A. S. Goldhaber, "Statistical Models of Fragmentation Processes," presented at High Energy Heavy Ion Summer Study, Lawrence Berkeley Laboratory, 1974.
9. J. Lepore and R. Riddell, in Proc. High Energy Heavy Ion Summer Study, Lawrence Berkeley Laboratory, 1974.
10. L. Bertocchi and D. Treleani, CERN-TH-2203, preprint (1976).
11. R. Blankenbecler, S. J. Brodsky and J. F. Gunion, Phys. Rev. D 6, 2652 (1972). See also D. Sivers, S. J. Brodsky and R. Blankenbecler, Physics Reports C 23, No. 1 (1976).

12. J. W. Cronin et al., Phys. Rev. Letters 31, 1426 (1973). J. W. Cronin et al., Phys. Rev. D 11, 3105 (1975).
13. S. D. Drell and T.-M. Yan, Ann. Phys. (N.Y.) 66, 578 (1971). G. West, Phys. Rev. Lett. 24, 1206 (1970).
14. R. Blankenbecler and S. J. Brodsky, Phys. Rev. D 10, 2973 (1974). For fixed angle counting rules see S. J. Brodsky and G. R. Farrar, Phys. Rev. Lett. 31, 1153 (1973); Phys. Rev. D 11, 1309 (1975).
15. We are generalizing and improving the hadron case treatment of C. Sachrajda and R. Blankenbecler (unpublished).
16. C. W. Akerlof et al., Phys. Rev. D 3, 645 (1971).
17. E. Gellent, LBL-784, preprint, Lawrence Berkeley Laboratory, presented at the Int. Conf. on Inclusive Reactions, Davis, California, 1972.
18. S. J. Brodsky and B. T. Chertok, Phys. Rev. D 14, 3003 (1976).
19. R. G. Arnold et al., Phys. Rev. Letters 35, 776 (1975). Lower energy data is taken from: J. Elias et al., Phys. Rev. 177, 2075 (1969); and S. Galster et al., Nucl. Phys. B32, 221 (1971).
20. A possible generalization that includes these effects is being studied in collaboration with A. Fernández-Pacheco.
21. See also the treatment of F. Gross, Phys. Rev. B 140, 410 (1965); William and Mary College preprint (March 1976). R. G. Arnold, C. E. Carlson, and F. Gross, Phys. Rev. Letters 38, 1516 (1977).
22. H. Moreno and J. Pestieau, Phys. Rev. D5, 1210 (1972); C. A. Dominguez and H. Moreno, Phys. Rev. D9, 2584 (1974).
23. W. B. Atwood and G. B. West, Phys. Rev. D7, 773 (1973).
24. P. V. Landshoff and J. C. Polkinghorne, Preprint DAMTP 77/2 (January 1977).

25. R. E. Taylor, in Proceedings of the 1975 International Symposium on Lepton and Photon Interactions at High Energies, ed. by W. T. Kirk (Stanford Linear Accelerator Center, Stanford University, Stanford, California, 1975), p. 679.

26. C. H. Llewellyn Smith, ibid., p. 709.

27. D. J. Gross and F. Wilczek, Phys. Rev. D 9, 980 (1974); 3633 (1973).

28. S. Coleman and D. J. Gross, Phys. Rev. Letters 31, 851 (1973). C. J. Callan and D. J. Gross, Phys. Rev. D 8, 4383 (1973). An interpretation of asymptotic freedom effects in terms of a generalized scale invariant parton model has been given by J. Kogut and L. Susskind, Phys. Rev. D 9, 3391 (1974).

29. W.-K. Tung, Phys. Rev. D 12, 3613 (1975).

30. A. DeRujula, H. Georgi, and H. D. Politzer, Ann. Phys. (N.Y.) 103, 315 (1977). H. D. Politzer, Coral Gables Conference, Florida, January 1977.

31. D. J. Gross, S. B. Treiman, and F. A. Wilczek, Princeton University preprint (October 1976).

32. R. Barbieri, J. Ellis, M. K. Gaillard, and G. G. Ross, Phys. Letters 64B, 171 (1976). R. K. Ellis, R. Petronzio, G. Parisi, Phys. Letters 64B, 97 (1976).

33. M. Chanowitz and S. D. Drell, Phys. Rev. Letters 35, 490 (1975). T. Kawabe, Kyushu preprint (June 1976).

34. E. M. Riordan et al., Stanford Linear Accelerator Center preprint SLAC-PUB-1634 (1975). See also J. S. Poucher et al., Phys. Rev. Lett. 32, 118 (1974). Data at small x (muon scattering) is from H. L. Anderson et al., Phys. Rev. Letters 38, 1450 (1977).

35. The small x fits were done in collaboration with J. A. Grifols.

36. W. B. Atwood et al., Stanford Linear Accelerator Center preprint SLAC-PUB-1758 (1976).

37. C. G. Callan and D. G. Gross, Phys. Rev. Letters 22, 156 (1969).

38. E. D. Bloom and F. J. Gilman, Phys. Rev. D 4, 2901 (1971).

39. G. B. West, Phys. Rev. D 14, 732 (1976).

40. O. Nachtmann, Nucl. Phys. B38, 397 (1972).

41. W. P. Schutz et al., Phys. Rev. Letters 38, 259 (1977).

42. V. Z. Jankus, Phys. Rev. 102, 1586 (1956). See also the discussion by L. Durand, III, Phys. Rev. 123, 1393 (1961).

43. E. B. Hughes, T. A. Griffy, R. Hofstadter, and M. R. Yearian, Phys. Rev. 146, 973 (1966).

44. L. L. Frankfurt and M. I. Strikman, Preprint LNPI-238, Leningrad (1976).

45. O. Nachtmann, Nucl. Phys. B63, 237 (1973). P. H. Frampton, Nuovo Cimento Letters 17, 499 (1976). For a review of generalized scaling variables see D. K. Choudhury, Tata preprint (February 1977).

46. M. J. Alguard et al., Phys. Rev. Letters 37, 1261 (1976).

47. D. J. Fox et al., Phys. Rev. Letters 33, 1504 (1974).
Y. Watanabe et al., Phys. Rev. Letters 35, 898 (1975).
H. L. Anderson et al., Phys. Rev. Letters 37, 4 (1976), and in Ref. 32.

48. S. J. Barish et al., ANL-HEP-PR-76-66. J. P. Berge et al., Phys. Rev. Letters 36, 639 (1976). H. Deden et al., Nucl. Phys. B85, 269 (1975). C. Cline, Proc. of the Palermo Conference on High Energy Physics, 1975. A fit to some of this data has been given by V. Barger et al., Nucl. Phys. B102, 439 (1976). Further tests have been presented by R. M.

Barnett and F. Martin, Stanford Linear Accelerator Center preprint SLAC-PUB-1892 (March 1977).

49. D. H. Perkins, P. Schreiner, and W. G. Scott, CERN preprint ANL-HEP-PR-77-16 (1977), submitted to Phys. Letters.

50. P. H. Frampton and J. J. Sakurai, preprint UCLA/77/TEP/3 (January 1977).

51. Applications of this model to neutrino reactions are being studied in collaboration with J. A. Grifols.